universität wien

MASTERARBEIT / MASTER'S THESIS

Titel der Masterarbeit / Title of the Master's Thesis

„The effect of prenatal methamphetamine exposure on glucose homeostasis in offspring"

verfasst von / submitted by

Maria Krassnitzer BSc

angestrebter akademischer Grad / in partial fulfilment of the requirements for the degree of

Master of Science (MSc)

Wien, 2018 / Vienna 2018

Studienkennzahl lt. Studienblatt / degree programme code as it appears on the student record sheet:	A 066 878
Studienrichtung lt. Studienblatt / degree programme as it appears on the student record sheet:	Masterstudium Verhaltens-, Neuro- und Kognitionsbiologie / Master's degree programme Behavior, Neurobiology and Cognition
Betreut von / Supervisor:	Univ.-Prof. Dr. Tibor Harkany

Affidavit

I declare that I have authored this thesis independently, that I have not used other than the declared sources/resources, and that I have explicitly indicated all material which has been quoted either literally or by content from the sources used. The text document uploaded to UNIVERSITY OF VIENNA online is identical to the present master's thesis.

July 2, 2018

Acknowledgement

I would first like to thank my thesis superviosr Prof. Tibor Harkany of the Department for Molecular Neurosciences at the Center of Brain Research. He gave me the great opportunity to be part and perform the practical part within his department.

I would also like to acknowledge Prof. Thomas Hummel of the Department for Neurobiology at the University of Vienna as being my internal mentor and additional reader of this thesis and I am thankful for his comments on this thesis.

With a great pleasure and much obliged I would like to mention Dr. Katarzyna Malenczyk. Dr. Malenczyk who is working on pancreas offered me this project I worked on and supervised me during my practical part and throughout the writing of my thesis. When we first met I didn't had much of experience in the techniques that the practical part encompassed. Despite this she was always optimistic, encouraging and motivating me all the time and brought out the best in me to finally receive this high quality of

work. The door to Dr. Malenczyk's office was always open whenever I had a question. I am very grateful that I had the chance to meet Dr. Malenczyk, a person with high professionality and great personality. I could not imagine to have any better teacher than you for this chapter of my educational way, I really appreciated to work with you.

Finally, I would like to express my very profound gratitude to my parents and to my partner, Gerhard and my three kids , Kilian, Levin and Elias for providing me with unfailing support and continuous encouragement throughout my years of study and through the process of researching and writing this thesis. You always believed in me and my competence. This accomplishment would not have been possible without them. Thank you.

Abstract

For glucose homeostasis the adequate secretion of insulin in a response to elevated glucose concentration in blood is necessary. Insulin is produced by and secreted from β-cells in the islets of Langerhans. It has been previously suggested that dopamine receptor 1 (DRD1) and dopamine receptor 2 (DRD2), dopamine transporter (DAT), vesicular monoamine transporter 2 (VMAT2), as well as dopamine itself are present in the β-cells of rodents. It was observed that dopamine signaling is affected by methamphetamine. We hypothesized that the treatment with methamphetamine at a specific time-point in embryonic development can affect the dopaminergic signaling pathway in endocrine pancreas and thus interfere with islet development and an adequate insulin secretion. We showed that the number of β-cells in 6 week old animals prenatally exposed to methamphetamine is significantly decreased. Moreover glucose tolerance test (GTT) showed that the level of glucose in the blood is elevated at baseline and throughout GTT in offspring prenatally exposed to methamphetamine. We further demonstrate that in methamphetamine treated INS-1E cells gene expression of *DRD1* is significantly decreased. Because the number of insulin positive β-cells is

Abstract

decreased in 6 week old animals prenatally exposed to methamphetamine we examined if it is due to apoptosis. Cleaved Caspase3 (Casp3) immunostaining showed that the number of apoptotic INS-1E-cells is significantly increased upon methamphetamine exposure. These findings reveal that methamphetamine affects the architecture of islets and gene expression of *DRD1* resulting in a non-adequate response to elevated blood glucose concentrations.

keywords: glucose homeostasis, islets of Langerhans, insulin, β-cells, dopamine receptor 1, dopamine receptor 2, dopamine transporter, vesicular monoamine transporter, Casp3, methamphetamine

Contents

List of Figures

List of Tables

Glossary

acyl-CoA acyl-Coenzyme A

alphaTC1 Alpha-tumor cell 1

Arx aristaless

ATP Adenosintriphosphat

AUC area under curve

BS blocking solution

BSA bovine serum albumin

Casp3 Cleaved Caspase3

CBD common bile duct

Cdk4 cyclin-dependent kinase 4

cDNA complementary DNA

CREB response element-binding protein

Cy Carbocyanine

DAG diacylglycerol

DAT dopamine transporter

DHAP dihydroxyacetone phosphate

DMEM Dulbecco's Modified Eagle's Medium

DRD1 dopamine receptor 1

DRD2 dopamine receptor 2

DRD3 dopamine receptor 3

DRD4 dopamine receptor 4

DRD5 dopamine receptor 5

ERK Extracellular signal-regulated kinase

FBS fetal bovine serum

Foxa2 forkhead box A2

G6P glucose-6-phosphate

Glut2 glucose transporter 2

Gly3P glycerol-3-phosphate

GSIS glucose stimulated insulin secretion

GTT glucose tolerance test

HBSS Hank's Balanced Salt Solution

HEPES hydroxyethyl piperazineethanesulfonic acid

Hes1 hairy and enhancer of split 1

i.p. intraperitoneally

IA1 insulinoma-associated 1

INS Insulinoma

Ki67 Kiel 67

L-Dopa L-3,4-dihydroxyphenylalanin

MafA musculoaponeurotic fibrosarcoma oncogene homolog A

MafB musculoaponeurotic fibrosarcoma oncogene homolog B

MAO monoamine oxidase

MM Mastermix

MMP Matrix metalloproteinases

NDS normal donkey serum

NeuroD1 Neurogenic differentiation 1

Ngn3 Neurogenin 3

NMDA N-methyl-D-aspartate

OCT optimal cutting temperature compound

Pax4 Paired box 4

Pax6 paired box 6

PB phosphate buffer

PCR polymerase chain reaction

Pdx1 pancreatic and duodenal homeobox 1

PFA paraformaldehyde

PKA protein kinase A

PVDF polyvinylidene difluoride

qPCR quantitative polymerase chain reaction

RIPA radioimmunoprecipitation assay

ROS reactive oxygen species

RPMI Roswell Park Memorial Institute

RT reverse transcription

S.D standard deviation

Tbp TATA-binding protein

TBS Tris-buffered saline

TCA tricarboxylic acid cycle

TGF transforming growth factor

VMAT2 vesicular monoamine transporter 2

1 Introduction

Ahmed (2002) writes in his review 'History of Diabetes Mellitus' that diabetes is a disease by which people all over the world can be affected. Some of its specific symptoms were already documented on the Ebers papyrus, which is over 3000 years old and was found in ancient Egypt. He further mentioned that the Indians noticed that symptoms associated with diabetes seem to be congenital or have a late onset and suggested a relation of the disease to heredity, obesity and diet. Araetus of Cappodocia first gave the term *diabetes*, which is a Greek word and literally means siphon. He described diabetes as a polyuric water disease. The Arab physician Avicenna first described the sweet taste of urine. [2]

In the more modern times two important approaches positively influenced the understanding of diabetes. First the usage of chemistry as a diagnostic tool and second the appearance of the endocrinology field in which Claude Bernard evidenced the ability of secretion of internal organs (glands). In the 17th century the concept of the sweetness of urine in diabetic patients came up again and the Latin word *mellitus*, meaning honey sweet, was attached. A century later it was confirmed that sugar is present in urine and blood of

the affected patients and that this is caused by a defect in the carbohydrate metabolism. [2]
Initially the pancreas was thought to be a gallbladder of spleen or to be necessary for the packing of stomach and adjacent organs. This hypothesis was disproved by the excision of dogs' pancreas. These operated animals showed excessive thirst and polyuria, symptoms associated with diabetes. [2]
Paul Langerhans discovered a population of pancreatic islet cells, which are embedded in the exocrine part of the pancreatic tissue. These groups of cells where later called the islets of Langerhans. The experiment with pancreateaomized dogs from Mering and Minkowski [39] showed that the islets play a crucial role in the carbohydrate metabolism. A few years later Laguesse suggested that the carbohydrate metabolism is regulated by a substance produced within and secreted from these cells. This substance was later called *insulin*, a Latin word for island, by Edward Sharpy-Shafer (1916) [28]. By the end of the 19th century the role of islets in energy homeostasis was established and their inadequate function linked to suffer from diabetes. It took 30 years more to finally discover, isolate and clinically use insulin. [2]

Dopamine a neurotransmitter in the central nervous system where it is produced and stored in the substantia nigra and the ventral tegmental area [38] was identified 1977 in isolated mouse islet homogenates by Hansen and Hedeskov [17]. Via the dopaminergic pathway dopamine can control crucial functions like behavior, cognition and reward. [38] It was reported that

drugs of abuse like cocaine negatively influence the dopaminergic pathway [25]. This drug has the ability to affect the dopamine level in the brain and interferes with DAT [25] and further influences the redistribution of VMAT2 in the rats striatum [14]. Brown et al. (2000) [9] showed that the vesicular dopamine uptake by VMAT2 was reduced by methamphetamine exposure. Methamphetamine known for its psychostimulant and addictive properties can decrease the level of dopamine within the brain. The administration of methamphetamine caused the formation of reactive oxygen species (ROS) that decreased the dopaminergic transporter function. [15]

1.1 Definition and Classification of diabetes

Diabetes comprises a group of metabolic disorders, which are characterized by defective insulin secretion in response to elevated blood glucose concentrations (*hyperglycemia*). [31]

The glucose metabolic disorders can be classified into four categories [31]:

- type1 diabetes mellitus that is characterized by the destruction of pancreatic β-cells
- type 2 diabetes mellitus that encompass decreased insulin secretion and sensitivity
- diabetes due to other specific mechanisms or diseases like genetic abnormalities or associated with other disorders and
- gestational diabetes mellitus

Depending on the degree of hyperglycemia the stage of glucose metabolism is categorized into a normal, borderline and diabetic. These stages are divided into a group of non-insulin and insulin-requiring for glycemic control and a group that is insulin-dependent for survival. [31]

1.1.1 Pancreas

The pancreas consists of an exocrine and endocrine part. Almost 95% of its mass counts to the exocrine compartment. The rest encompasses the endocrine pancreas, islets of Langerhans, which play a relevant role in the synthesis, storage and secretion of insulin by β-cells, glucagon by α-cells, somatostatin by δ-cells and pancreatic polypeptide by PP-cells. [4]

1.1.2 Pancreas development

The development of the pancreas can be divided into three main stages (Fig.1.1). The first stage is called primary transition and lasts from embryonic day E9.5 to E12.5, a secondary transition from E13.5 till birth and a third period of development from birth till weaning. [4]
The primary transition of the pancreatic development comprises the thickening of the endoderm and its expansion. Within this period the formation of a pancreatic bud and the expression of different transcription factors like *pancreas-specific transcription factor (Ptf1), pancreatic and duodenal homeobox 1*

(Pdx1), *sry-box 9 (Sox9)* and others by a subset of epithelial cells, occur. [4]
The formation of microlumen results from the proliferation of epithelial cells. These microlumens coalesce and form tubular structures. At the point of tube formation the structure is divided into two domains. On top of the tubule there is a tip domain consisting of multipotent progenitor cells whereas the trunk domain consists of bipotent progenitor cells. There are the multipotent pancreas-specific transcription factor positive (+) ($Ptf1^{+}$) progenitors that give raise to endocrine, duct and acinar cells and the bipotent Nkx6.1 homebox+ ($Nkx6^{+}$) progenitors that differentiate into duct and endocrine cells. [4]
During secondary transition pancreatic branching, cell differentiation and the formation of islets are crucial events for pancreas morphogenesis (Fig.1.1). [4]

Islet development

During the secondary transition a subset of endocrine cells from the trunk region express transiently *Neurogenin 3 (Ngn3)* (Fig.1.2). Its expression is controlled by the Notch signaling pathway and the inactivation of hairy and enhancer of split 1 (Hes1), a Notch pathway constituent, that leads to the repression of *Ngn3* expression.[32]

Ngn3 is expressed as early as E9.5 but its expression is relatively low until the secondary transition. Then Ngn3 level increases to promote differentiation of five endocrine cell types. [32]

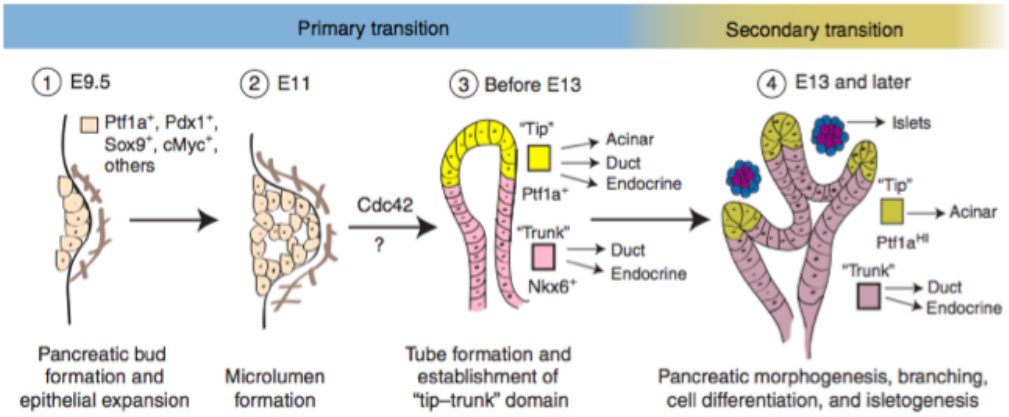

Figure 1.1: **The pancreatic development and crucial transcription factors during the primary and secondary transition.** The primary transition with the formation of a pancreatic bud and the proliferation of epithelial cells followed by the formation of microlumen and through its coalescence the build up of tubular structures characteristic for pancreatic morphology. In panel 1 there are epithelial cells expressing mainly *pancreas-specific transcription factor (Ptf1)*, *pancreatic and duodenal homeobox 1 (Pdx1)*, *sry-box 9 (Sox9)*, *cMyc*. The formation of microlumen by proliferating epithelial cells is shown in panel 2. In panel 3 in yellow the tip domain giving raise to acinar, duct and endocrine cells and in pink the trunk domain giving raise to duct and endocrine cells is shown. Panel 4 demonstrates the secondary transition with morphogenesis, cell differentiation and the formation of islets. The cells within the tip domain lose their multipotency and give raise just acinar cells whereas the progenitors of the trunk domain retain their bipotency. [4]

Cells expressing *Ngn3* delaminate from the epithelia, migrate and coalesce into polyclonal clusters (Fig.1.2). The formed clusters at E13.5 and later are called the islets of Langerhans. [4]
The $Ngn3^{+}$ progenitor cells can differentiate into all five endocrine cell types α, β, δ, PP (pancreatic polypeptide) and ϵ cells. Grapin-Botton and coworkers showed that the development of the endocrine cell types is temporally regulated with α-cells formed first followed by β and δ cells. At last the PP expressing cells arise. [4] Islets of Langerhans show a characteristic arrangement of its cell types with β-cells in the center of the islet surrounded by α, δ and PP cells. [4]

The transcription factor *insulinoma-associated 1 (IA1)* is expressed in insulinoma and pancreatic β-cells, as well as in human embryonic pancreas and mouse nervous system. [22] Studies from Mellitzer et al. (2006) [22] showed that Ngn3 induces and regulates *IA1* gene. It is further assumed that *IA1* can influence a proper formation of α and β-cells. [22] Another transcription factor Neurogenic differentiation 1 (NeuroD1), also plays a critical role in differentiating and mature endocrine cells as such, mice with NeuroD1 deficiency revealed the formation of hypoplastic, disorganized islets. [32]

α-cell development

A variety of transcription factors, such as paired box 6 (Pax6), forkhead box A2 (Foxa2) and aristaless (Arx) are crucial for α-cell development (Fig.1.3A). Mutations in Pax6 result in lack of α-cells and lead to reduced expression

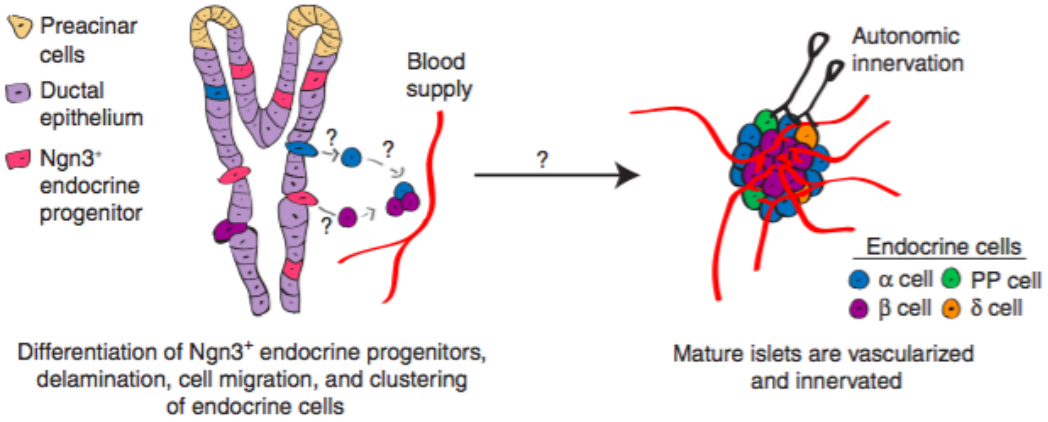

Figure 1.2: **Formation of an islet by the differentiation of the Ngn3 endocrine progenitors into either α, β, δ or PP cells.** Differentiation is followed by delamination of endocrine cells and their aggregation into cell clusters with an islet-specific cell arrangement. [4]

of glucagon. On the other hand the transcription factor Arx is not only necessary for α-cell maturation but also for the maintenance of adult α-cells.[4] It has been shown that Arx null mutants lack α-cells [12] but reveal an increase in β and δ-cell numbers [4]. Therefore, this transcription factor is necessary for α-cell fate acquisition and the suppression of β-cell fate [32].

β-cell development, maturation and proliferation

Paired box 4 (Pax4) and Nkx2.2 (Fig.1.3A) are two out of a variety of transcription factors that play a crucial role in the differentiation of Ngn3+ progenitors to β-cells. During early endocrine differentiation *Pax4* and *Arx*

are co-expressed and both mutually and directly affect α and β-cell fate. [32]
During the early postnatal period the immature β-cells start sensing glucose allowing them to regulate insulin secretion. [4] Yet, these β-cells are functionally immature, which means that their ability to synthesize and secrete insulin is reduced. Due to their low O_2 consumption they show a non-oxidative metabolism. Expression of the *glucose transporter 2 (Glut2)* and the ability to cleave proinsulin to insulin are important steps in β-cells maturation. [32]

Both the musculoaponeurotic fibrosarcoma oncogene homolog A (MafA) and musculoaponeurotic fibrosarcoma oncogene homolog B (MafB) regulate β-cells maturation. MafA is only found in β-cells from E13.5 onward and important to activate insulin transcription (Fig.1.3B). In contrast *MafB* is expressed in β-cells as well as α-cells from E12.5 but postnatally its expression is restricted to α-cells. [32]

Two key regulators for β-cells maturation are *Pdx1* and *NeuroD1* that demonstrate increase in expression levels between birth and weaning (Fig.1.3B). The postnatal inactivation of pancreatic and duodenal homeobox 1 (Pdx1) results in reduced β-cell function and the early onset of diabetes. [4] Also the lack of NeuroD1 in β-cells results in a decrease in insulin secretion and the cell function resembling that of immature β-cells.
After maturation β-cells show a transient burst of proliferation (Fig.1.3C). A variety of cell cycle regulators are involved in this process e.g. cyclin-

dependent kinase 4 (Cdk4) or D-type cyclins (CcnD1 and CcnD2). p16, p19 and p27, cyclin-dependent inhibitors, have been identified to regulate β-cell mass expansion. [4]

1.1.3 Vascularization and innervation of the islet

At the point of maturation islets are vascularized and innervated by the autonomic nervous system (Fig.1.2). [4]
Islets form dense networks with blood vessels and receive a higher amount of blood than cells in the adjacent exocrine tissue. The capillaries contain of a large number of pores called *fenestrae*, that allow unrestricted access to nutrients as well as expeditious insulin diffusion into the blood. [16]

1.2 Insulin

Insulin is a peptide hormone that is synthesized and secreted by β-cells in response to glucose. [16] First reports of the monomeric structure of insulin appeared in 1926 by John Abel [1]. Only four centuries later the zinc-containing hexameric structure of insulin was described. [6]
Insulin exhibit three conformations:

- monomeric
- dimeric
- hexameric

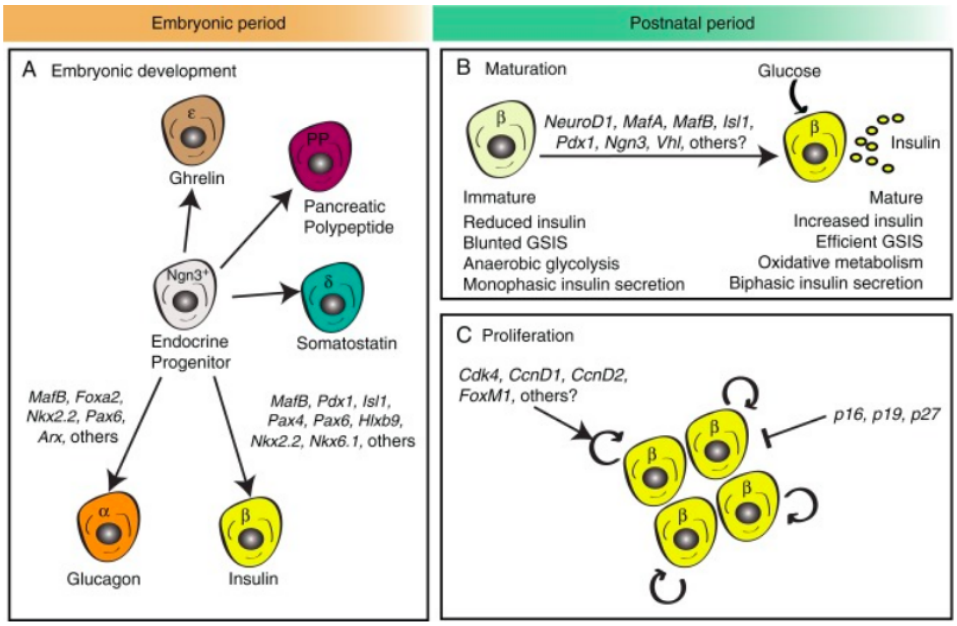

Figure 1.3: **Embryonic and postnatal period of endocrine cell development.** In panel A endocrine progenitor cells expressing *Ngn3* differentiate into the five endocrine cell types. The expression of certain transcription factors results in the differentiation into distinct lineages. α-cells secreting glucagon, β-cells secreting insulin, δ-cells secreting somatostatin, ϵ-cells secreting ghrelin and PP-cells secreting pancreatic polypeptide. In the postnatal period (B and C) the maturation and proliferation of β-cells induced by transcription factors like NeuroD1, MafA, MafB, Pdx1 and others is demonstrated. β-cell proliferation is regulated by cell cycle regulators (Cdk4, CcnD1) and inhibited by cyclin-dependent inhibitors p16, p19 and p27.[4]

The conformation is influenced by the concentration of insulin and the surrounding pH. Monomers can form dimers or hexamers if the required amount of insulin concentration, pH and zinc are available. In the hexameric structure insulin is packed into dense core granules and stored in the β-cells. [16]
Insulin is secreted in its hexameric conformation and only upon diffusion into the blood, due to electrostatic repulsion and the decreased concentration it dissociates into the monomeric state. Hence insulin is in its active state. [16]

1.2.1 Glucose-induced insulin secretion

Glucose is a principle component in food and its level in blood can raise immediately after food intake. The insulin secretion induced by glucose compared to fatty acids or protein is markedly higher. When glucose concentration in the blood increases it is taken up by β-cells via glucose transporter 2 (Glut2). Glut2 is the only glucose transporter being expressed in β-cells.[16]
The activation of Glut2 occurs in an insulin-independent manner. When glucose enters the cytosol via the transporter the monosaccharide is phosphorylated into glucose-6-phosphate (G6P) by the enzyme glucokinase in the first step of glycolysis (Fig.1.4). Aim of glycolysis is to gain pyruvate that can be further used in the tricarboxylic acid cycle (TCA) for the oxidative metabolism in the mitochondria to obtain Adenosintriphosphat (ATP). The

increasing ATP levels in the cytosol induce the closure of K_{ATP} channels that lead to the depolarization of the cell membrane and thus the opening of voltage-dependent Ca^{2+} channels. The influx of Ca^{2+} induces exocytosis of insulin-containing granules. [16]
Another metabolic pathway of glucose is the metabolization of G6P into dihydroxyacetone phosphate (DHAP) to provide glycerol-3-phosphate (Gly3P) (Fig.1.4). Gly3P can augment insulin secretion by generating diacylglycerol (DAG) and long-chain acyl-Coenzyme A (acyl-CoA). [16]

Insulin secretion shows a biphasic pattern consisting of a rapid spike in insulin release called the first phase and a decline with a sustained second phase that remains throughout the duration of the stimulus. [16]

1.3 Dopamine

Dopamine is a crucial neurotransmitter in the central nervous system but also plays an important role in non-neuronal tissues.[38] The precursor of dopamine L-3,4-dihydroxyphenylalanin (L-Dopa) and dopamine itself are present in small concentrations in the plasma. This circulating peripheral dopamine can not pass the blood-brain barrier thus not interfere with the brain dopamine activity. [38] It functions in a paracrine manner within the tissue where it is synthesized. It can affect blood pressure, liquid clearance through the alveolar epithelium in the lungs and reveals its protective role on the intestinal mucosa in the gastrointestinal duct. [38] Its activity has

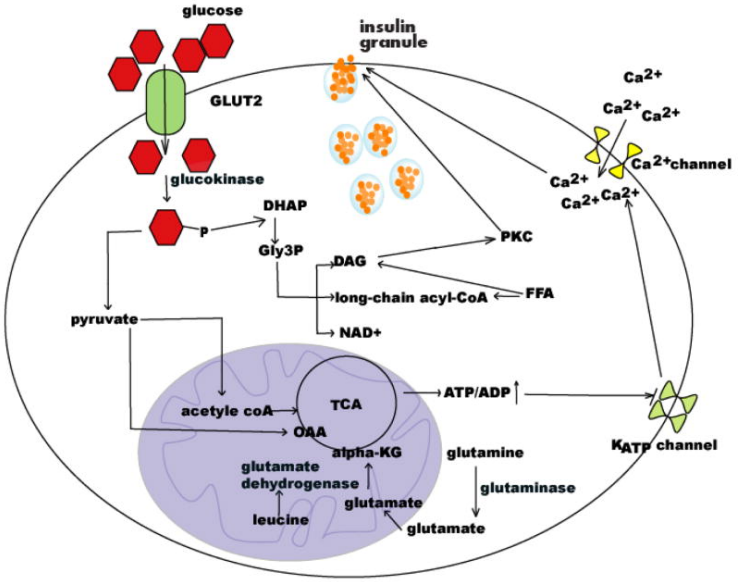

Figure 1.4: **Mechanism of insulin secretion induced by glucose, amino acids and free fatty acids (FFA).** Glucose enters β-cells via Glut2 and is phosphorylated by glucokinase. Glycolysis is the stepwise reduction of monosaccharides like glucose with pyruvate being its endproduct. Pyruvate is further metabolized to acetyl-Coenzyme A (acetyl-CoA) or Oxalacetate (OAA). Both enter the TCA cycle in the mitochondria of β-cells and produce ATP from products of the TCA. The elevated ATP level in the cell causes the closure of K_{ATP} channels. It leads to the depolarization of cell membrane and subsequent opening of voltage-dependent Ca^{2+} channels. The influx of Ca^{2+} induces exocytosis of insulin-containing granules. Additionally phosphorylated glucose can be metabolized to DHAP that is further metabolized to Gly3P. The products generated by Gly3P metabolism are long-chain acyl-CoA and DAG, which also stimulate insulin secretion. DAG activates protein kinase C (PKC) that further affects insulin secretion. Insulin secretion is also regulated by glutamine and leucine. Glutamine is converted into glutamate via glutaminase. Leucine activates glutamate dehydrogenase, which converts glutamate into α-ketoglutarate (alpha-KG) that enters the TCA cycle and causes ATP production thus enhancing insulin secretion. FFA serve for synthesis of DAG and long-chain acyl-CoA. DAG then activates PKC that is involved in insulin secretion. Long-chain acyl-CoA acylate synaptogamin and synaptosomal-associated protein-25 (SNAP-25) that are crucial in insulin granule fusion with the plasma membrane.[16]

been also demonstrated in the pancreas. [38]

1.3.1 Dopamine signaling within β-cells

Five types of dopamine receptors exist. They are divided into 2 families depending on their protein structure and function. The dopamine receptor 1 (DRD1) and dopamine receptor 5 (DRD5) belong to one group and are called D1-like receptors. The dopamine receptor 2 (DRD2), dopamine receptor 3 (DRD3) and dopamine receptor 4 (DRD4), which show homology in structure and function are classified as D2-like receptors. [38]
Depending on the type of receptor that it binds to, dopamine exhibits its specific effects within the tissue. The D2-like receptors were found in β-cells of mice and shown to decrease protein kinase A activity in β-cells. Further D2-like receptors can activate phospholipase C and increase intracellular Ca^{2+} level in medium spiny neurons. [38]
Beside the receptors β-cells express monoamine oxidase (MAO) and aromatic L-amino acid decarboxylase, which converts L-dopa into dopamine. [38] β-cells in rodents show expression of *vesicular monoamine transporter 2 (VMAT2)* and *dopamine transporter (DAT)*, components necessary for dopamine secretion. [38] VMAT2 takes up dopamine from the cytosol into vesicles to protect from neurotransmitter oxidation by MAO. DAT takes up dopamine from the extracellular space into the cytosol. [38]

1.3.2 Regulation of insulin secretion via dopamine signaling

Ericson et al. (1977) [13] observed that mice injected with L-Dopa revealed an accumulation of dopamine in pancreatic β-cells and that dopamine accumulation results in an improper secretion of insulin. Rubi et al. (2005) proved the presence of D2-like receptors in mice and found *DRD2* receptor expression on secretory insulin granules of mice. They demonstrated that dopamine treatment caused an increase in ATP levels and suggested this results as a consequence of reduced ATP consumption because mitochondrial activation was not affected. Further Rubi et al. (2005) showed that INS-E cells exposed to dopamine exhibit reduced cytosolic Ca^{2+} levels, necessary for secretory response. [29] Dopamine binding to another member of the D2-like family, DRD3, inhibits glucose stimulated insulin secretion (GSIS) by decreasing (Ca^{2+})i oscillation (Fig. 1.5). Within the β-cell MAO can oxidize dopamine. Dopamine can be taken up by VMAT2 into vesicles to protect the neurotransmitter from MAO activity. Dopamine can then be co-secreted with insulin as demonstrated in Figure 1.5. [38] The D2-like receptors within the pancreatic endocrine tissue can negatively regulate cAMP production and decrease protein kinase A (PKA) activity in pancreatic β-cells. This decreased PKA activation can affect divers targets including ion channels (Ca^{2+} channels), the cAMP response element-binding protein (CREB) and ionotropic glutamate channels resulting in impaired signaling. [38]

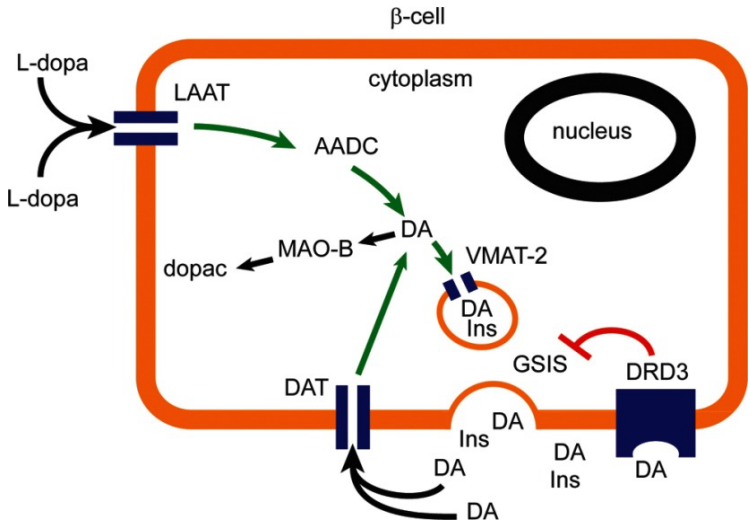

Figure 1.5: **The machinery of the dopaminergic signaling pathway within a β-cell.** Circulating L-Dopa enter the β-cell of pancreatic islet via Lysosomal amino acid transporter (LAAT). Due to decarboxylation of L-Dopa by aromatic L-amino acid decarboxylase (AADC) inside the cell dopamine (DA) is synthesized. Dopamine is either sequestered into vesicles by VMAT2 or metabolized by monoamine oxidase (MAO) into 3,4-dihydroxyphenylacetic acid (dopac). DAT take up DA from the extracellular space. DA is co-secreted with insulin (Ins) due to GSIS and inhibits GSIS by binding to the D_3 as well. [38]

1.4 Methamphetamine

Methamphetamine is an artificial drug of abuse and acts on dopamine signaling by enhancing the activities of the dopaminergic system. [26]
This drug of abuse enters the cytosol of β-cells by serving as a substrate for DAT. Interestingly, methamphetamine has the ability to reverse the activity of DAT from an influx to an efflux of dopamine. In a healthy organism dopamine is pumped into vesicles against a proton gradient. Methamphetamine promotes the release of stored dopamine from the vesicles through its interaction with reserpine sites on the VMAT2 as well as by the disruption of the vesicular proton gradient. [26]
Additionally methamphetamine inhibits the metabolism of dopamine by MAO. As a consequence of the elevated dopamine concentration in the cytosol induced by methamphetamine, dopamine is available to reverse the action of DAT and stimulate dopamine receptors. [26]

As previous studies on fetal nicotine exposure [10] and prenatal caffeine exposure [34] in rats showed that nicotine as well as caffeine affects glucose homeostasis and revealed increased apoptosis of pancreatic β-cells.

With these previous findings we wanted to investigate if and how the exposure of pregnant mice to methamphetamine at a specific point in embryonic development affects β-cell formation and thus insulin secretion in the offspring.

2 Materials & Methods

2.1 Injection of mice

All animals were kept under standard housing conditions with a 12-h/12-h light/dark cycle and food and water available *ad libitum*. Experiments on live animals conformed to the European Communities Council Directive (86/609/EEC) were approved by regional ethical committees and regulated by applicable local laws (Tierversuchsgesetz 2012, BGBI, Nr. 114/2012, Austria). Particular effort was directed towards minimizing the number of animals used and their suffering during experiments. The intraperitoneal injection of pregnant C57BL6/J mice (n= 4 per treatment) at E14.5 was performed with methamphetamine (10 mg/kg body weight) or saline that served as a control for the following 3 days.

2.2 Collection, fixation, freezing and cryosectioning of pancreas

Mice were sacrificed at birth (P0) or at the age of 6 weeks. P0 bodies or pancreas from 6 week old mice were fixed in 4% paraformaldehyde (PFA) for 24 h at 4°C and afterwards PFA was replaced with 30% sucrose containing 0.1% sodium azide as a preservative. Subsequently the bodies and pancreas were embedded into a cryomold with optimal cutting temperature compound (OCT) (Tissue-Tek® O.C.T.™ Compound). The tissue was frozen either on dry ice or liquid nitrogen. The freezing process with liquid nitrogen was faster and the sample did not curl up as much as by freezing on dry ice. Snap freezing in general reduces the chance of water forming ice crystals in the tissue. The bodies and pancreata were cut sagittally on the cryostat (Leica CM1860 UV) at -20°C in 14 μm sections and tissue was picked up onto SuperFrost^{+}glass slides.

2.3 Immunohistochemistry for insulin, glucagon, DAT, DRD2 and VMAT2

To localize and identify insulin, glucagon, DAT, DRD2 and VMAT2-positive cells in pancreatic islets, tissues were immunolabeled with specific antibodies (Table 2.6). Selected slides were labeled and tissue sections were

bordered with Dako pen. Each section was rinsed for 10 min with 0.1 M phosphate buffer (PB) (77.4 ml 0.1 M Na_2HPO_4 and 22.6 ml 0.1 M NaH_2PO_4 diluted to 1 L with distilled H_2O, pH= 7.4) and blocked with the blocking solution (BS) (10% normal donkey serum (NDS), 5% bovine serum albumin (BSA), 0.3% Triton X in 0.1 M PB) for 2-3 h at room temperature. After the blocking step the sections were incubated with select primary antibodies in 5% NDS, 0.2% BSA, 0.3% Triton X in 0.1 M PB for 48 h at 4°C. The primary antibodies solution was removed and the tissues rinsed once with 0.1 M PB followed by three washing steps for 10 minutes each. After washing the tissues were incubated with Carbocyanine (Cy) conjugated secondary antibodies (Cy2 anti-guinea pig 1:300, Cy5 anti-mouse 1:500, Cy3 anti-rabbit 1:300 in 2% BSA in 0.1 M PB), nuclei were counterstained with *Hoechst* 33342 (Sigma) (1: 1,000) for 2 h at room temperature. The secondary antibodies solution was removed and the slides were washed 3-4 times for 30 min with 0.1 M PB. Before mounting, the sections were rinsed once with milliQ water and subsequently mounted with Dako mounting medium.

2.4 Cell culture of INS-1E and αTC1-6 cells

INS-1E cell line derived from rat insulinoma and displays characteristic features of pancreatic β-cells. This cell line shows a high insulin content and glucose response [33]. Alpha-tumor cell 1 (alphaTC1)-6 cells derived from mouse adenoma and revealed high levels of glucagon mRNA [27]. INS-1E cells were cultured in Roswell Park Memorial Institute (RPMI)-1640 medium

(Sigma R0883) containing Gluatmax (100X), hydroxyethyl piperazineethane-sulfonic acid (HEPES) (10 mM), heat-inactivated fetal bovine serum (FBS) (5%), sodium pyruvate (1 mM), antibiotics (100 μg/mL streptomycin, 100 IU/ml penicillin) and β-mercaptoethanol (50 μM) in the incubator (Thermo Scientific, HERAcell VIOS 160i CO_2 Incubator) at 37°C. αTC1-6 cells were cultured in Dulbecco's Modified Eagle's Medium (DMEM) low glucose (1 g/L) medium (Gibco 31885-023) supplemented with HEPES (15 mM), heat inactivated FBS (10%), BSA (0.02%), non-essential amino acids (0.1 mM), sodium bicarbonate (1.5 g/L), glucose (2 g/L) and antibiotics (100 μg/mL streptomycin, 100 IU/mL penicillin). INS-1E and αTC1-6 (ATCC) cell lines were cultured in T25 flask until 90% confluent (~6 mln cells/T25 flask) and then split to gain 1 mln cells/T25 flask. For this old medium was removed and replaced with 500 μl of 0.5% trypsin to detach cells from the surface of the flask. After 1 minute incubation and tapping, cells were detached. The old medium was filled into the flask and finally transferred into a 50 ml falcon tube to centrifuge at 1200 rpm for 3 min. The supernatant was discarded and pellet was resuspended in 6 ml of appropriate fresh medium.

2.5 Immunocytochemistry of INS-1E and αTC1-6 cells

To examine cell proliferation in saline versus methamphetamine treated cells antibody against Kiel 67 (Ki67), a nuclear protein expressed in proliferating cells, was used. For the examination of cell death Cleaved Caspase3 (Casp3), a marker for apoptosis, was used. Additionally cells were co-stained for DAT. A 24-well plate with 12-mm coverslips coated with 0.001% poly-D-lysine (Sigma) was put under UV-light for 1 h and finally INS-1E and αTC1-6 cells were plated into the plate. After incubation poly-D-lysine was removed and washed with milliQ water. Next day cells were treated for 48 h with 5 μM methamphetamine or saline (as a control). For Immunocytochemistry medium was removed and cells were washed in 0.1 M PB and fixed in 4% PFA (0.1 M PB) for 15 min at room temperature. The PFA was removed and cells rinsed with 0.1 M PB prior exposure to a blocking solution composed of 0.1 M PB, 10% NDS, 5% BSA, 0.3% Triton for 2 h at room temperature on the shaker followed by overnight incubation with the primary antibodies (Table 2.6) in BS (0.1 M PB, 5% NDS, 0.2% BSA, 0.3% Triton) at 4°C. Next cells were washed 3 times for 10 min on the shaker and then incubated with Cy-conjugated secondary antibodies (Cy 2-donkey-anti–rabbit and Cy 3-donkey-anti-guinea pig in 0.1 M PB) for 2 h at room temperature on the shaker. Nuclei were counterstained with *Hoechst* 33342 (Sigma) (1: 1,000). Subsequently cells were washed 3 times for 20 min in 0.1 M PB. Three coverslips per slide were mounted and imaged with the 20X objective on

the confocal microscope (Zeiss LSM800).

2.6 Glucose tolerance test and isolation of pancreatic islet

2.6.1 Glucose tolerance test

This test was performed to determine if animals prenatally exposed to methamphetamine or saline exhibit an alteration in glucose metabolism. Offspring (6 weeks old) of mothers treated with saline or methamphetamine (n = 16 saline, n = 16 methamphetamine) were used for this experiment. Mice were separated the day before into single cages and fast overnight with water available *ad libitum*. Each mouse was weighed to calculate the amount of glucose solution that has to be injected (20% glucose solution in dH_2O at room temperature sterilized with syringe filter 0.2 μm).

After one night of starvation the test started in the morning with the measurement of the baseline value. For this, the tail tips of the mice were cut off. The first drop of blood was discarded and the second drop collected with a strip of the FreeStyle Lite glucometer (Abbott Diabetes Care). Next the mice were injected intraperitoneally (i.p.) with the filtered glucose solution (2 g glucose/kg body weight.). To measure blood glucose level

Solutions (per 6 mice)	
Buffer Q (HBSS + 10% FBS)	**Buffer D**
11 ml FBS	0.75 ml 1M HEPES
100 ml HBSS	30 ml HBSS

Table 2.1: Components and volumes of buffer Q and buffer D solution used for islet isolation

at 15, 30, 60, 90 and 120 minutes after i.p. removal of the first drop and collection of the second drop with a strip of glucometer were repeated.

2.6.2 Isolation and culture of pancreatic islets

The isolation of pancreatic islets is to obtain viable purified islets. To acquire such pancreatic islets from methamphetamine and saline treated offspring the sacrificed animal went through a pancreatic perfusion with collagenase that releases islets from exocrine tissue [11]. To prepare stock solution of collagenase type I, 25 mg/ml lyophilized collagenase (Sigma) was warmed up to room temperature and dissolved in 4 ml of Hank's Balanced Salt Solution (HBSS) then kept on ice for 30 min and mixed from time to time. Afterwards the collagenase stock solution was aliquoted into 120 μl/tube and kept at -20°C.

The mice used for GTT were sacrificed to collect islets. This procedure was

conducted under the hood. Mice were put into a covered glass beaker and anesthetized with isoflurane (Forane®) and sacrificed by cervical dislocation. The body was fixed on a polystyrene box and sprayed with ethanol. To expose the abdominal cavity mice were cut by midline excision. After this the gallbladder, the bile duct as well as the small intestine were exposed and clamped with mosquito clamps (Fig.2.1) on both sides of the opening of common bile duct (CBD) to the duodenum to close it.

Pancreas was perfused by injecting 3 ml of cold and freshly prepared working solution of collagenase (0.3 mg/ml) in buffer D (Fig.2.1), into the gallbladder (Fig.2.2) using a 30G needle and 5 ml syringe. After perfusion clamps were removed and pancreas dissected. Pancreata that were not totally perfused were cut into small pieces to facilitate enzymatic digestion. Four pancreata from the same treatment (methamphetamine or saline) were placed into a 50 ml falcon tube containing working collagenase solution (2 ml per tissue).

For digestion the pancreata were incubated for 15-20 min at 37°C water bath. To ensure the disruption of the tissues, tubes were vigorously shaken. Afterwards the tubes were filled up to 50 ml with cold buffer Q (Fig.2.1) to stop enzymatic reaction – centrifuged at 1200 rpm (4°C, 1.5 min) and the supernatant was removed. The acquired pellet was suspended in 10 ml buffer Q. Undigested tissue or single cells were removed by filtering (pore size sieve -1mm). The sieve was rinsed once more with 20 ml of buffer Q. To collect islets and wash away cells the digested tissue suspension was transferred onto a strainer (pore size 70 μm). At this point the islets

Figure 2.1: Abdominal cavity of mouse. Mosquito clamps clamping the CBD at the duodenum. (in YouTube^{AT} 2011; Web 28 Oct 2017) [36]

remain on the strainer. By moving the strainer upside down the islets on the strainer were washed with 10 ml of RPMI-1640 medium supplemented as above into a petri dish. Islets (Fig.2.3) were cultured overnight at 37°C or hand picked for glucose stimulated insulin secretion. Under the light microscope 10 islets/1.5 ml tubes were collected in 500 μl RPMI-1640 medium supplemented as above.

2.7 Confocal microscopy and cell counting

The stained tissues were imaged on a confocal microscope (Zeiss LSM800) at 5X, 20X or 40X/1.4 water immersion objective magnification for further quantitative analysis. Images were acquired in the Zen 2.1 software. To avoid artifacts and background the laser intensity was adjusted. Finally the

Figure 2.2: Perfusion of pancreas through the CBD.(in YouTube^{AT}2011; Web 28 Oct 2017) [36]

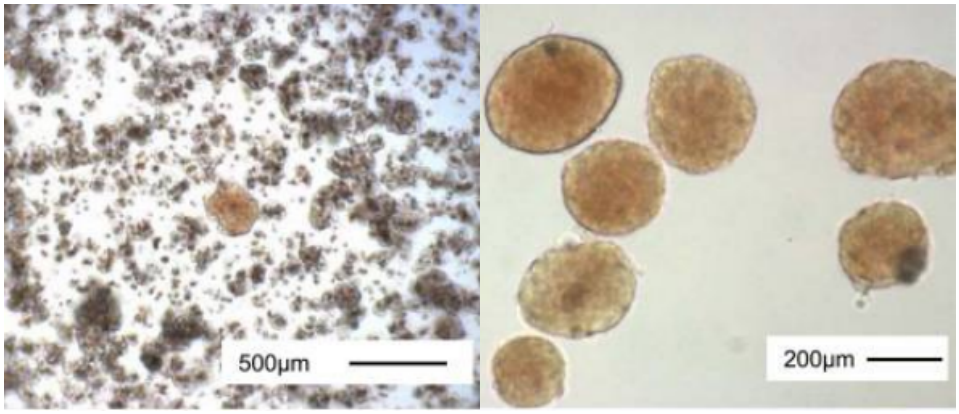

(a) (b)

Figure 2.3: Islet within acinar tissue (a) and purified islets (b). [11]

images were converted in tif-format to quantify in imageJ-win64 software. The quantification parameters for saline and methamphetamine samples comprised the expression pattern of insulin and glucagon-positive cells. We counted insulin and glucagon expressing cells within and outside of bigger cell clusters (pancreatic islets). Pancreata from P0 were used to determine the effect of prenatal exposure to methamphetamine on islet size. To quantify number of proliferating and apoptotic cells, INS-1E and αTC1-6 cells positive for Ki67 and Casp3 respectively were counted and numbers were normalized to total number of nuclei.

2.8 Western blot of INS-1E for DAT

To examine protein level of DAT, cultured INS-1E cell line were treated with 5 μM methamphetamine or only with RPMI-1640 medium supplemented as above, which served as a control. First the old medium was removed and replaced by either medium or medium supplemented with the drug and incubated for 48 h at 37°C. After incubation the cells were scrapped off the wells and transferred into a 50 ml falcon tube. The tubes were centrifuged at 1200 rpm for 3 minutes. The supernatant was discarded and the acquired pellet suspended in radioimmunoprecipitation assay (RIPA) buffer (1% TritonX, 150 mM NaCl, 10 mM NaF, 50 mM Tris, 5 mM EDTA, 1X proteases inhibitors and 5 mM Na_3VO_4) vortexed consistently within 30 min and stored on ice. The samples were spin down for 5 min at 4500 rpm (4°C) and the supernatant was used for electrophoresis. For this 20 μl

of sample supplemented with 20 μl Amersham WB Loading buffer (1:1) and Cy 5 (1:100) were boiled at 95' for 5 min. In each well either a volume of 40 μl of sample or 30 μl of Amersham WB molecular weight marker (1:100) or PageRuler™ Prestained Protein ladder 1:50 (ThermoFisher) were pipetted. Before the transfer the tissues were wetted in transfer buffer and the polyvinylidene difluoride (PVDF) membrane activated in methanol and then rinsed in transfer buffer to increase its protein binding capacity. Transfer buffer (100 ml Tris-buffered saline (TBS) 1X: 50 mM Tris-HCl, pH 7.6; 150 mM NaCl; 200 ml methanol; 700 ml dH_2O) was prepared and proteins transferred from the gel onto PVDF membrane (Fig.2.4). The blocking step was performed in 3% BSA (in TBS 1X) for 30 min followed by an overnight incubation with primary antibody solution (Table 2.6) at 4°C on the shaker. The next day primary antibody solution was removed and membrane washed 3 times for 5 min in TBST (TBS 1X+ Tween 1:1,000). The membrane was incubated for 1 h with Cy 3- conjugated secondary antibody (anti-rabbit 1: 2500 in 3% BSA). Next It was washed 2 times in TBST for 5 min followed of a final wash in TBS 1X for 5 minutes. Before the scan (Fig.2.4) the membrane was dried.

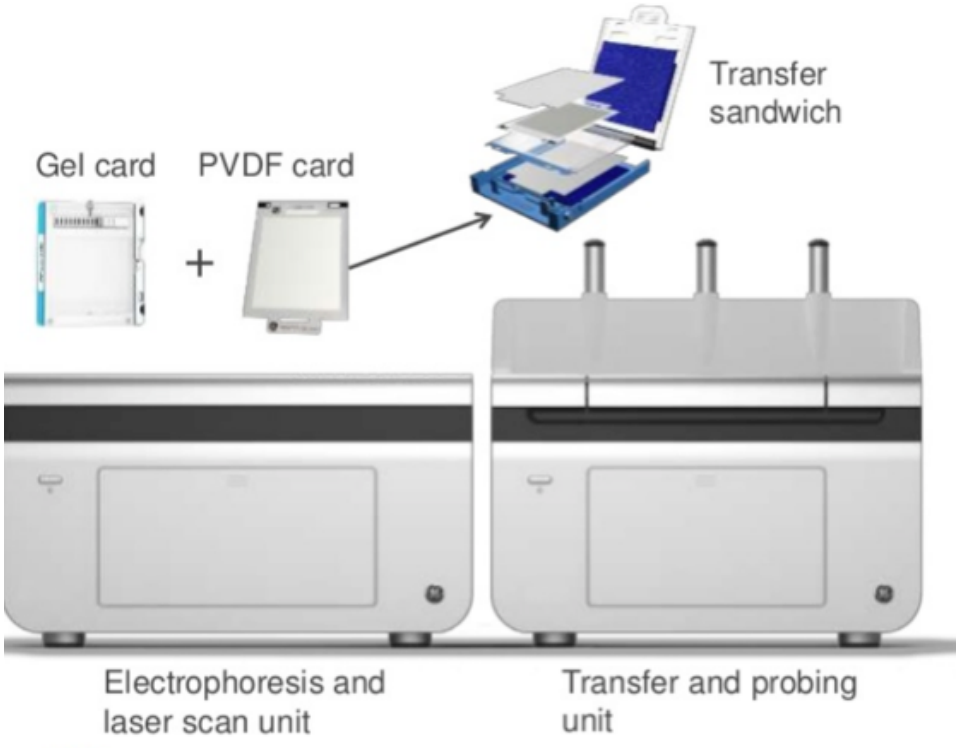

Figure 2.4: Western blot set up for electrophoresis, transfer and scan. Transfer sandwich consisting of holder, sponge, filter paper, gel, membrane, filter paper and 2 sponges. (in SlideShare LinkedIn Corporation©2018; Web 11 Nov 2017) [40]

2.9 Polymerase chain reaction and quantitative polymerase chain reaction

To test gene expression of *DAT*, *DRD1* and *DRD2* in INS-1E and αTC1-6 cells we performed PCR and qPCR.

2.9.1 RNA extraction, reverse transcription and quantitative polymerase chain reaction

RNA extraction from INS-1E and αTC1-6 cells was performed according to the user guide Lexogen Split RNA Extraction Kit for Phenol-Chloroform Extraction. The concentration of RNA was measured with the Nanodrop. An A260/230 ratio of around 2 guarantied the purity of isolated RNA. RNA was used for reverse transcription (RT) to gain complementary DNA (cDNA). The Applied Biosystems™ High-Capacity cDNA Reverse Transcription Kit (Mastermix (MM) consisting of 10X RT buffer, 25X of dNTP Mix, 10X RT random Primer, multi Scribe RT and nuclease free water) was prepared. RT was performed as demonstrated in Table 2.2. To perform quantitative polymerase chain reaction (qPCR) cDNA (INS-1E: meth: 346,2 ng/μl; saline: 539,2 ng/μl and αTC1-6: meth: 316 ng/μl; saline: 69,5 ng/μl) and MM (SybrGreen, final concentration of 5 μM forward and reverse Primer, nuclease free water) for each primer were prepared. The 96-well plate was filled up with a triplicate of each gene of interest and the samples as well as

Table 2.2: Program for reverse transcription (RT)

23°C	37°C	85°C	4°C
10′	2°	5′	∞

with a reference gene (*TATA-binding protein (Tbp)*) for normalization. qPCR was conducted with Bio-Rad CFX Connect™ Real-Time System.

2.9.2 Primers of DAT, DRD2 and DRD1 amplification from INS-1E, αTC1-6 and mouse islets

Mouse specific primers for DAT, DRD2 and rat specific primers for DRD1 (Table 2.3) were used to conduct polymerase chain reaction (PCR). The selected primers (20 μM) were added to the MM (Table 2.4) to conduct PCR. cDNA from INS-1E, αTC1-6 cells and islets (100 ng/μl) was prepared by RT (High-capacity cDNA Reverse Transcription Kit; Applied Biosystems) from previously extracted total RNA (Lexogen Split RNA Extraction Kit for Phenol-Chloroform Extraction). PCR was performed as demonstrated in Table 2.5 in Thermal Cycler Bio-Rad T100. PCR products (10 μl of sample with 1 μl 10X Loading Dye) were resolved on a 1.5% agarose gel. Electrophoresis was conducted for 30-45 min at 120V. Gel was supplemented with 1:10,000 GelRed. The gel was imaged with Bio-RadChemiDoc™ XRS and analyzed with Image Lab™ Software.

Table 2.3: List of primers used for PCR

Gene	Primer sequence
DAT	Forward: 5′- CTA CAT GGA GCT GGC TCT CG-3′
	Reverse: 5′- GAA GCC CAC ACC TTT CAG GA-3′
DRD1	Forward: 5′- GCA TGG CTT GGA TTG CTA CG-3′
	Reverse: 5′- CCA GTT GCT GCC TGG ACT AA-3′
DRD2	Forward: 5′- GAC ACC ACT CAA GGG CAA CT-3′
	Reverse: 5′-TCC ATT CTC CGC CTG TTC AC-3′

Table 2.4: Components and volumes of the Mastermix for 25 μl total volume

cDNA	H_2O	Primer fw	Primer rev	2x PCR
1.5 μl	10 μl	0.5 μl	0.5 μl	12.5 μl

Table 2.5: PCR program used for DAT and DRD2

94°C	94°C	59°C	72°C	go to 2	72°C	12°C
4′	30″	30″	45″	39X	5′	∞

Table 2.6: List of antibodies used for immonocytochemistry, immunohistochemistry and Western blot

Antibody	Host species	Concentration	Source
Cleaved caspace 3	Rabbit	1:700	Cell Signaling
DAT	Guinea-pig	1:750 (cytochemistry)	Synaptic System
DAT	Rabbit	1:500 (histochemistry)	Synaptic System
DAT	Rabbit	1:500 (Western blot)	Synaptic System
DRD2	Rabbit	1:500	Gift from K.Mackie
Glucagon	Mouse	1:1,000	Sigma
Insulin	Guinea-pig	1:500	Cell Signaling
Ki67	Rabbit	1:600	Santa Cruz
VMAT2	Rabbit	1:500	Synaptic System

2.10 Statistics

For insulin-positive β and glucagon-positive α-cell quantifications, calculations of cells from Po (n = 8 methamphetamine; n = 8 saline) and 6 week (n = 7 methamphetamine; n = 4 saline) old animals prenatally exposed to methamphetamine and saline, were conducted. To quantify islets per area, n = 6 islets per mouse, from Po (n = 4 methamphetamine; n = 4 saline) and, $n > 4$ islets per mouse, from 6 week old offspring (n = 7 methamphetamine; n = 4 saline) the number of islets were normalized to the labeled area of the pancreas tissue. The calculated average of α and β-cells per islets of each animal was used for statistical analysis. For the quantification of the GTT

animals at the age of 6 weeks were used (n = 16 methamphetamine; n = 16 saline). Determination of glucose clearance during the GTT was obtained by the calculation of the area under curve (AUC). The mean value of Ki67 and Casp3 positive-cells were normalized to the mean value of cells stained for Hoechst. For Western blot protein of interest was normalized to total protein. Statistical analysis for qPCR was conducted by double Δ-Ct analysis and expression level of *DRD1* and *DRD2* were normalized to the housekeeping gene encoding *Tbp*. All data were expressed as means ± standard deviation (S.D). Statistical significance was determined by t-test and were considered significantly different at $p < 0.05$.

3 Results

3.1 Immunoreactivity of insulin and glucagon-positive cells in mouse pancreas

To examine the effect of prenatal exposure to methamphetamine on insulin and glucagon-positive cell number of insulin and glucagon-positive cells in the endocrine part of pancreas over time, immunhistochemical analysis of P0 (Fig.3.1) and 6 week old offspring (Fig.3.3) prenatally exposed to methamphetamine or saline, were conducted. Immunohistochemical analysis show the distinct pattern of cell clusters where glucagon-positive α-cells surround insulin-positive β-cells (Fig. 3.1a). Furthermore single α and β-cell immunoreactivity is demonstrated in Fig.3.1b. Considering these observations our quantitative analysis of cell-counting in P0 pancreata focused on α and β-cell clusters at both age as well as on single cells. Data from cell counting showed no significant difference neither for insulin-positive cells from P0 ($p \approx 0.2738$) nor for glucagon-positive cells ($p \approx 0.6913$) from P0 and 6

week old offspring ($p \approx 0.2374$) as demonstrated in Fig.3.2a, Fig.3.2b and Fig.3.3d. A significant decrease ($p < 0.001$) in β-cell number with ≈ 25 cells per cluster is given for mice prenatally exposed to methamphetamine compared to control with a cell number of ≈ 41 cells per cluster (Fig.3.3c). The mean value of insulin-positive β-cells in P0 pancreata from saline treated mothers is ≈ 25 cells per cluster and for methamphetamine it is ≈ 19 cells per cluster. P0 pancreata contain ≈ 3 glucagon-positive α-cells per cluster in offspring prenatally exposed to methamphetamine and saline, respectively (Fig.3.2a; 3.2b). For the pancreas from 6 week old mice the mean value of glucagon-positive α-cells is ≈ 11 cells per cluster for animals prenatally exposed to saline and ≈ 8 cells per cluster for animals prenatally exposed to methamphetamine. Quantification of single glucagon-positive α-cells scattered in the exocrine tissue from P0 mice, cells revealed no significant difference ($p \approx 0.9593$) between methamphetamine exposed and control group, with a mean value of ≈ 3 cells per section for each treatment. There is no significant difference in number of single insulin-positive β-cells ($p \approx 0.2770$) in progeny from saline (≈ 8 cells per pancreas) or methamphetamine (≈ 6 cells per section) treated mothers (Fig.3.2c; Fig.3.2d).

3.1 Immunoreactivity of insulin and glucagon-positive cells in mouse pancreas

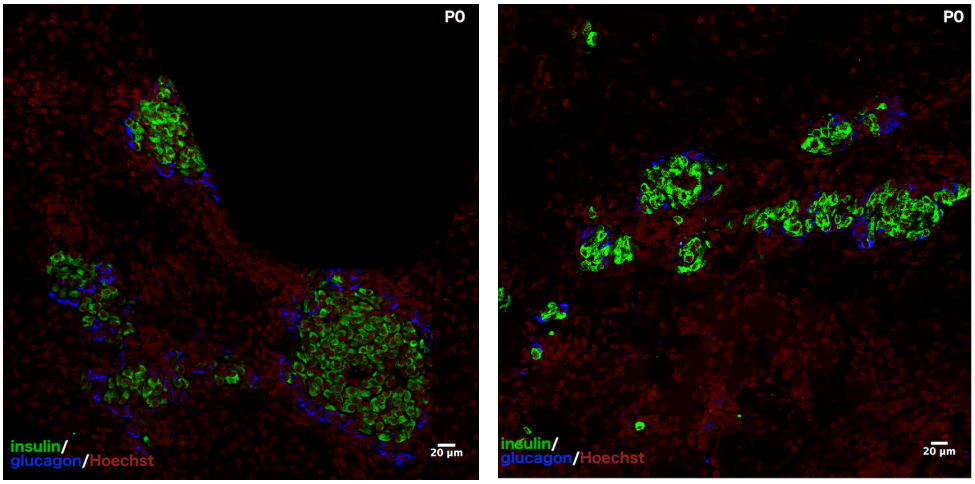

(a) (b)

Figure 3.1: Representative confocal images of pancreatic tissue of P0 mice in 20X magnification are shown (a,b). Immunosignal in green is positive for insulin and in blue positive for glucagon. Nuclei were stained with Hoechst (pseudocolored in red). Immunostaining revealed clusters of insulin positive β-cells surrounded by glucagon positive α-cells in pancreas from animals prenatally exposed to saline (a) and methamphetamine (b). The number of islets in (a) is lower compared to the number of islets in (b). Both images (a,b) confirm the presence of glucagon-positive α and insulin-positive β single-cell distribution in pancreas. Scale bars 20 μm.

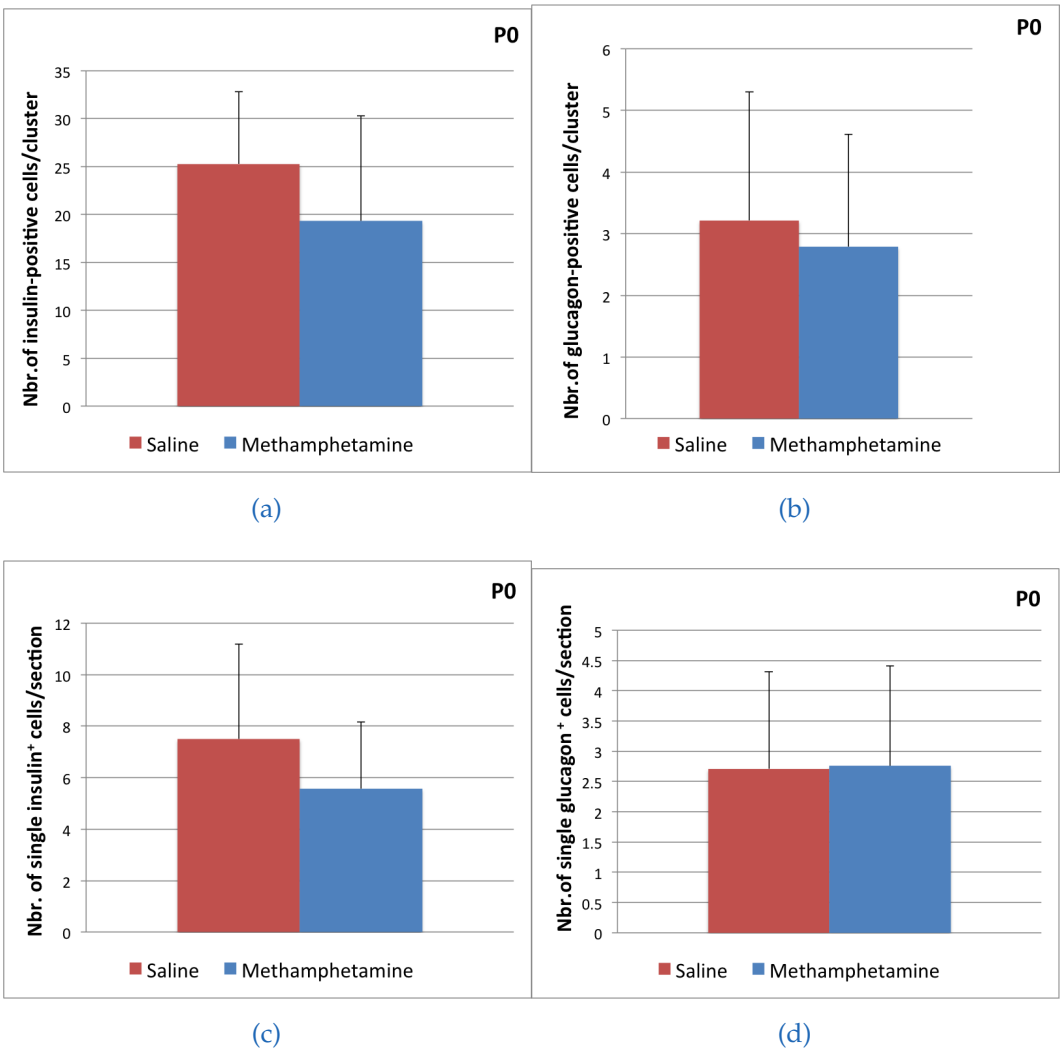

Figure 3.2: Quantification of insulin and glucagon-positive cells in P0 mice revealed no significance in number of glucagon-positive α and insulin-positive β-cells within clusters (c, d). The quantification from single cell distribution of glucagon-positive α and insulin-positive β-cells revealed no significant difference. Data are expressed as means ± S.D, statistical analysis was obtained by t- test. For saline and methamphetamine n = 8 mice/group were analyzed.

3.1 Immunoreactivity of insulin and glucagon-positive cells in mouse pancreas

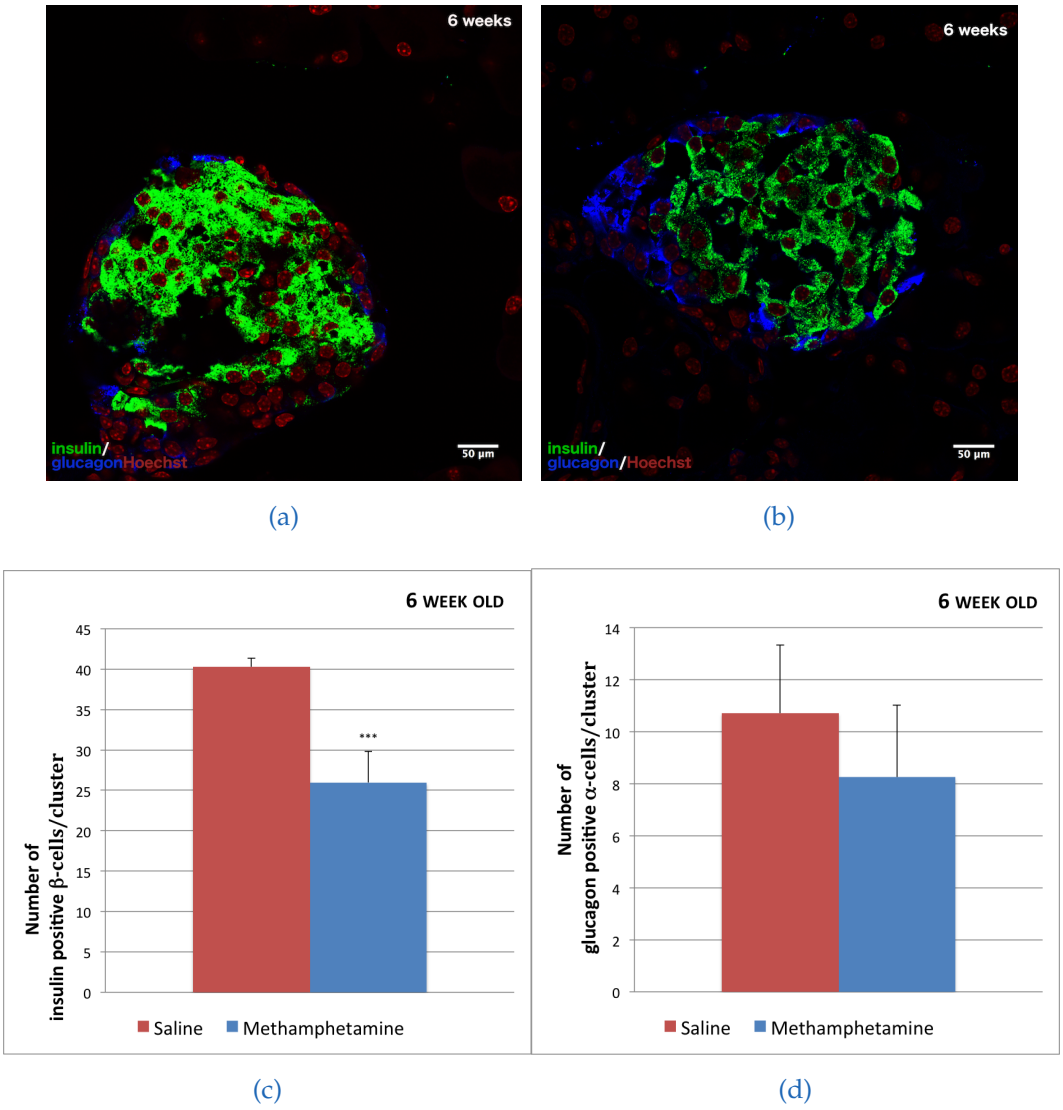

Figure 3.3: Representative confocal images in 40X magnification of islets from 6 week old offspring from mothers treated with saline (a) and methamphetamine (b). In green insulin-positive β-cells and in blue glucagon-positive α-cells are demonstrated. Nuclei were stained with Hoechst (pseudocolored in red). Islets show the typical structure with insulin-positive β-cells in the center that are surrounded by glucagon-positive α-cells. The quantification of insulin-positive β-cells within the clusters revealed a significant difference in cell number of animals prenatally exposed to methamphetamine compared to control. Data are expressed as means ± S.D, statistical analysis was obtained by t- test. ***P <0.001. n=7 mice prenatally exposed to methamphetamine and control n=4 were analyzed. Scale bars 50μm.

3.2 Number of islets is methamphetamine dependent

During cell counting of glucagon-positive α and insulin-positive β-cells from P0 mice and 6 weeks old a difference in islet numbers between offspring from saline and methamphetamine treated mice was observed. To validate this observations pancreata from P0 and 6 week old mice were immunostained for insulin where clusters of insulin-positive β-cells indicate islets as demonstrated in Fig.3.4 and Fig.3.5. The quantification of insulin-positive β-cell clusters from P0 revealed no significant difference in the number of islets between animals prenatally exposed to saline or methamphetamine ($p \approx 0.1261$; Fig.3.4c). The mean value of islets is ≈ 7 islets per mm^2 in P0 prenatally exposed to saline and ≈ 12 islets per mm^2 in offspring from mothers treated with methamphetamine. 6 week old offspring prenatally exposed to methamphetamine with a mean value of ≈ 0.9 islets per mm^2 showed significantly increased ($p < 0.01$) numbers of islets per area compared to offspring from saline treated mothers with a mean value of ≈ 0.6 islets per mm^2.

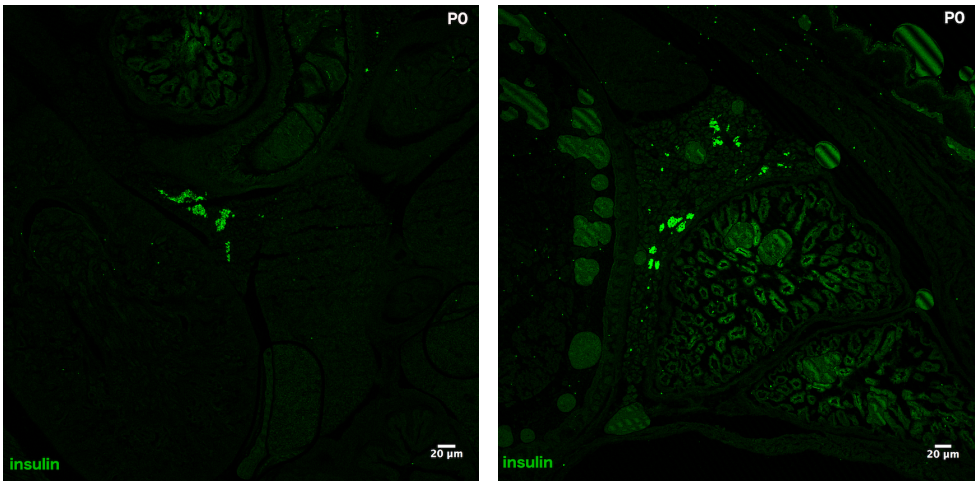

(a) (b)

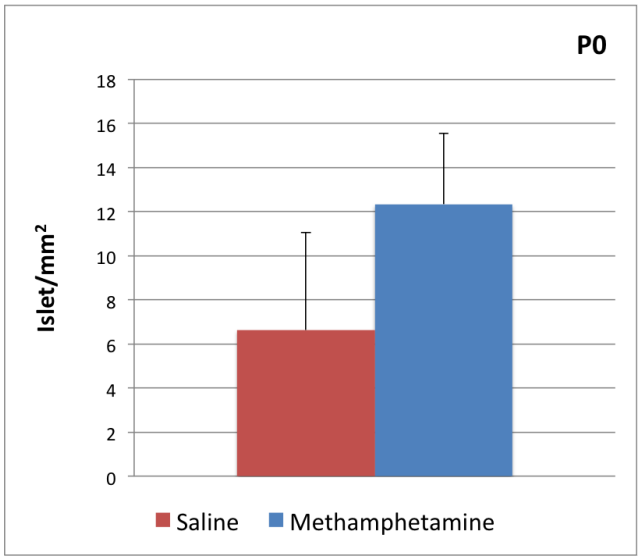

(c)

Figure 3.4: Representative confocal images from P0 mice islets (cell clusters) in 5X magnification of mice prenatally exposed to saline (a) and methamphetamine (b). In green is shown insulin indicating islet distribution. Green autofluorescence shows exocrine part of pancreas as well as adjacent organs. Quantification revealed no significant difference in the number of islets (c). Data are expressed as means ± S.D, n = 4 mice per treatment; statistical analysis was obtained by t-test. Scale bars 20μm.

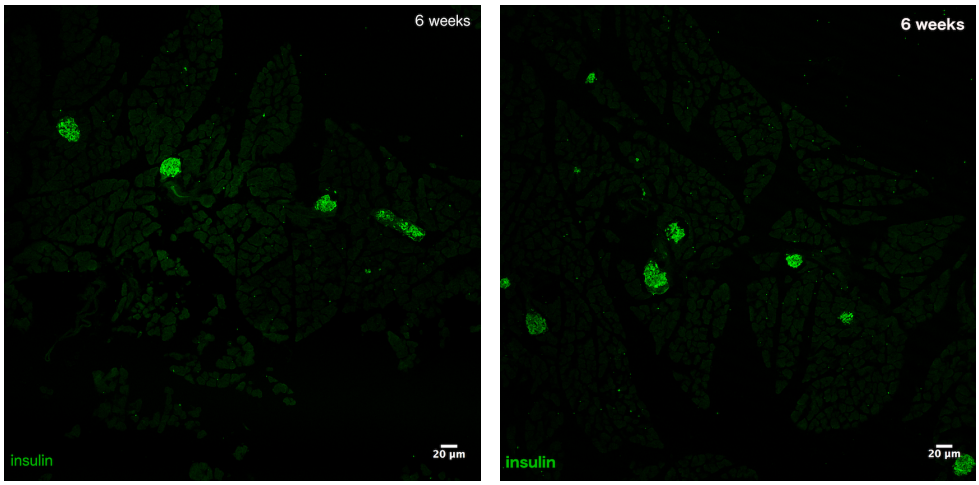

(a) (b)

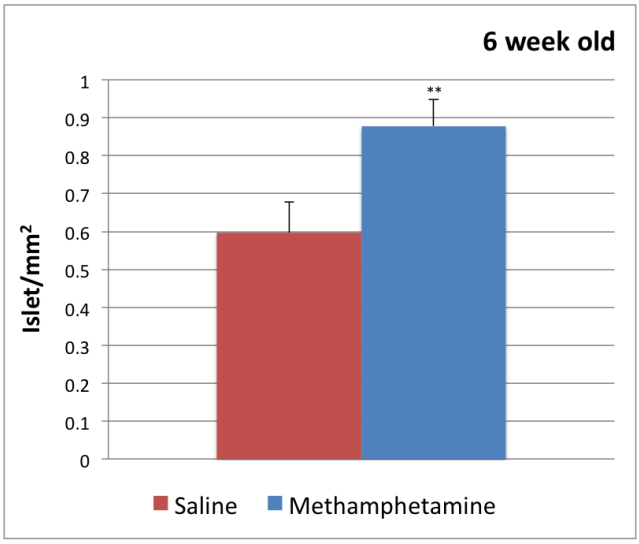

(c)

Figure 3.5: Representative confocal images of pancreatic islets from 6 week old offspring in 5X magnification and with a 0.6 Zoom. Immunosignal of insulin-positive cells is shown in green. Cell clusters reveal islets. Green autofluorescence shows exocrine part of pancreas. Quantification revealed a significant increase in number of islet per mm^2 (c) in animals prenatally exposed to methamphetamine. Data are expressed as means ± S.D, n = 4 mice per treatment; statistical analysis was obtained by t-test. **P <0.01. Scale bars 20μm.

3.3 Apoptosis is markedly higher in methamphetamine treated INS-1E cells

Because quantifications revealed a significant difference in the number of β-cells in clusters as well as in the number of islets in 6 week old offspring from methamphetamine treated mothers we wanted to investigate if this is the results of cell proliferation or apoptosis. To examine if methamphetamine can affect cell proliferation or cell death of insulin secreting cells, immunocytochemistry in INS-1E cell line was conducted. Proliferating cells were identified by staining for Ki67 (Fig.3.6a; Fig.3.6b) and cells undergoing cell death were identified by staining for Cleaved Caspase3 (Fig 3.7a; Fig.3.7b). Cells positive for Ki67 or Casp3 were normalized to total amount of stained nuclei. Quantification of saline ($\approx$ 0.0504 % for $Ki67^+$ cells) and methamphetamine ($\approx$ 0.0336 % for $Ki67^+$cells) treated INS-1E cells revealed no significant change in $Ki67^+$ INS-1E cells ($p \approx 0.4829$) as shown in Fig.3.6c. Apoptosis of INS-1E cells is significantly increased ($p < 0.05$) in cells treated with methamphetamine with a mean number of 0.0914 % for $Casp3^+$ cells. The control group of INS-1E cells shows a mean number of 0.0258 % for $Casp3^+$ cells (Fig.3.7c). Analysis of proliferation and apoptosis of αTC1-6 cells revealed no significant difference between cells treated with methamphetamine compared to control ($\approx$ 0.6134 % for $Ki67^+$ and $\approx$ 0.1885 % for $Casp3^+$ cells; Fig. 3.8; Fig.3.9).

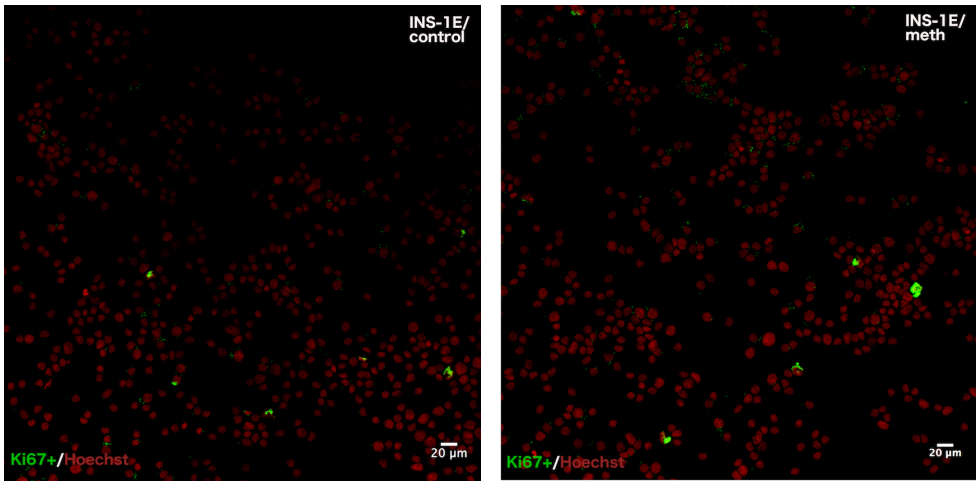

(a) (b)

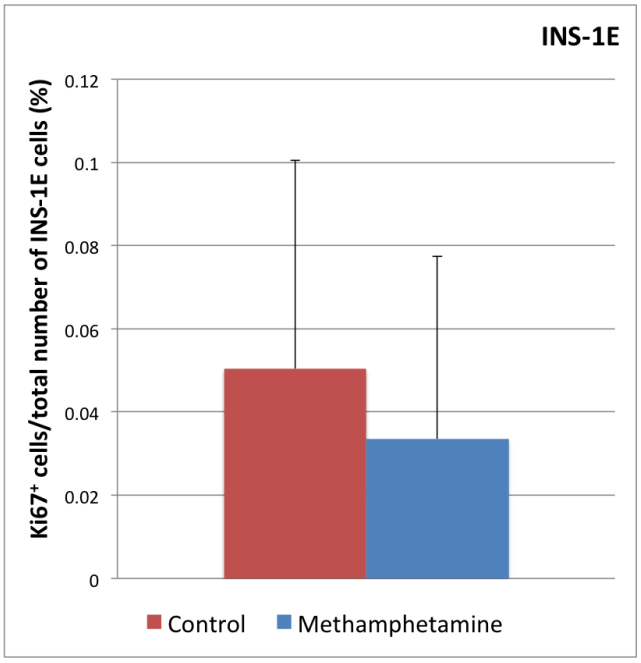

(c)

Figure 3.6: Representative confocal images of INS-1E cells in 20X magnification. The control group is shown in (a) and the methamphetamine treated cells are shown in (b). Immunosignal in green indicate Ki67-positive cells (a,b). Nuclei were stained with Hoechst (pseudocolored in red). Number of Ki67-positive cells was normalized to the total number of stained nuclei. Data are expressed as means ± S.D and statistical analysis was obtained by t-test. n = 3 coverslips per treatment. Scale bars 20μm.

3.3 Apoptosis is markedly higher in methamphetamine treated INS-1E cells

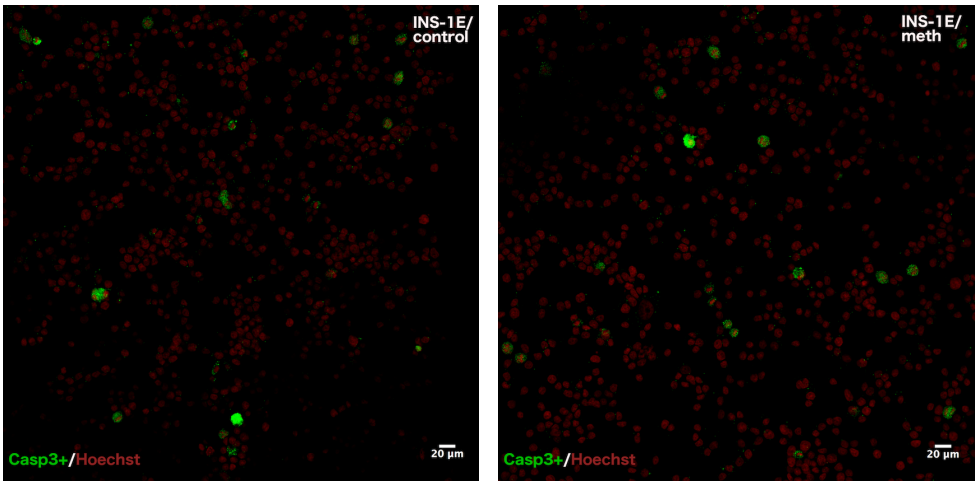

(a) (b)

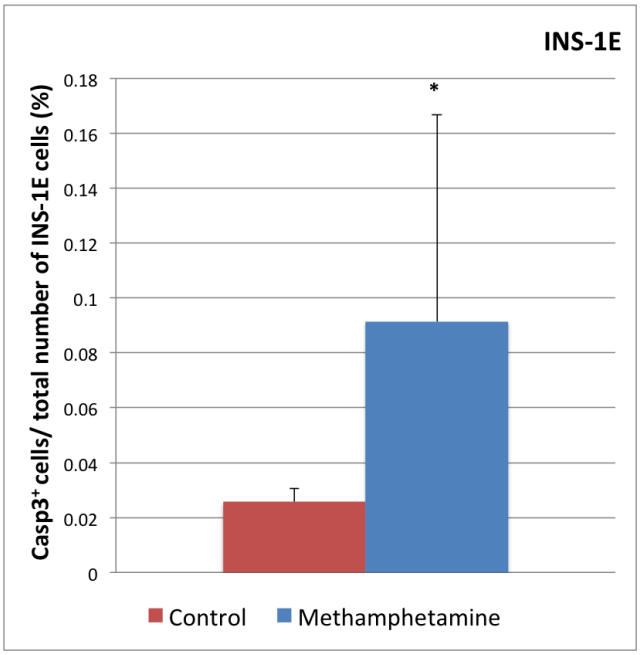

(c)

Figure 3.7: Representative confocal images of INS-1E cell in 20X magnification. The control group is shown in (a) and the methamphetamine treated cells are shown in (b). Immunosignal in green indicate Cleaved Caspase3-positive cells (a,b). Nuclei were stained with Hoechst (pseudocolored in red). Analysis of cell death (c) revealed a significant number of apoptotic INS-1E cells after exposure methamphetamine. Casp3-positive cells were normalized to total number of stained nuclei. Data are expressed as means ± S.D and statistical analysis was obtained by t- test, *P <0.05. n = 3 coverslips per treatment. Scale bars 20μm.

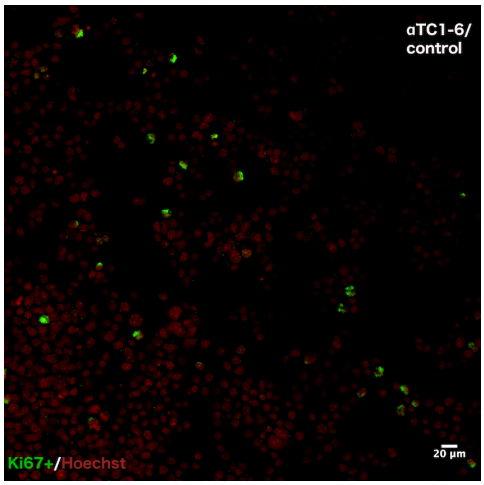

(a)

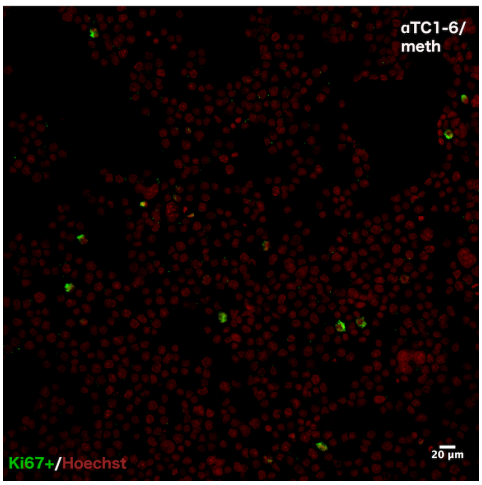

(b)

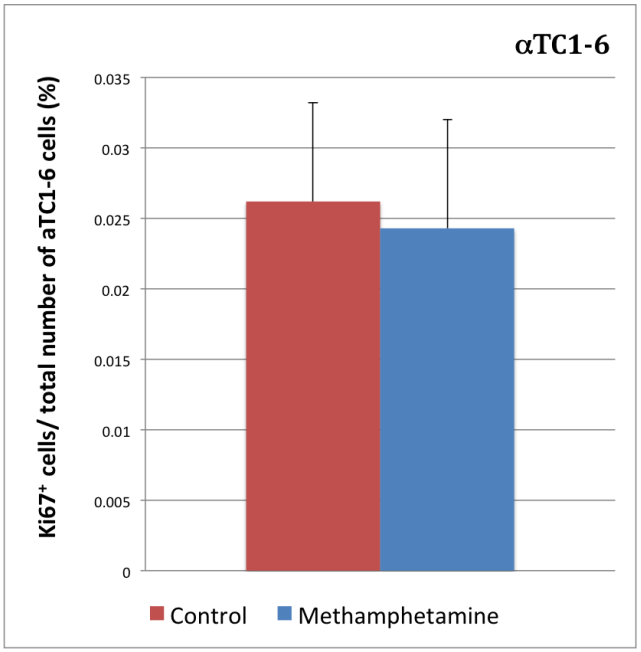

(c)

Figure 3.8: Representative confocal images of αTC1-6 cells in 20X magnification. The control group is shown in (a) and the methamphetamine treated cells are shown in (b). Immunosignal in green indicates Ki67-positive cells (a,b). Nuclei were stained with Hoechst (pseudocolored in red). Quantification revealed no significant difference in cell proliferation between methamphetamine and control (c). Ki67-positive cells were normalized to total number of stained nuclei. Data are expressed as means ± S.D and statistical analysis was obtained by t- test. n = 3 coverslips per treatment. Scale bars 20μm.

3.3 Apoptosis is markedly higher in methamphetamine treated INS-1E cells

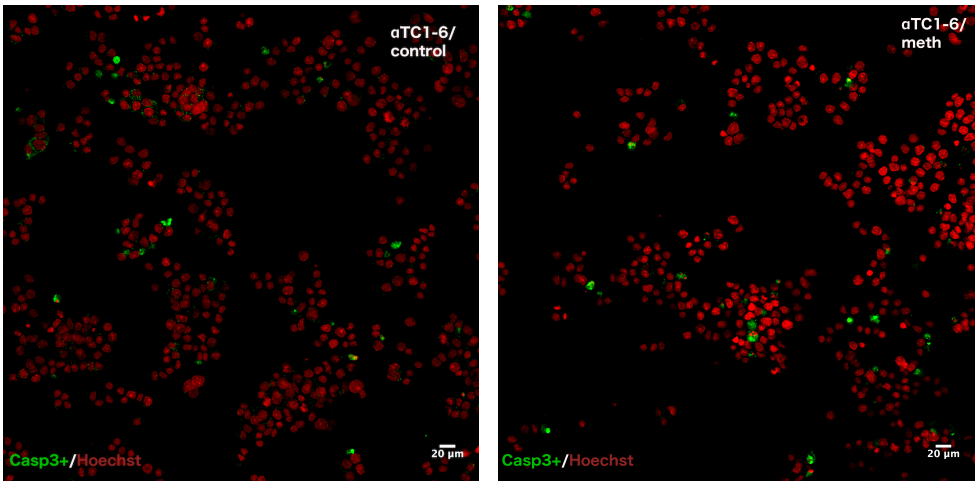

(a) (b)

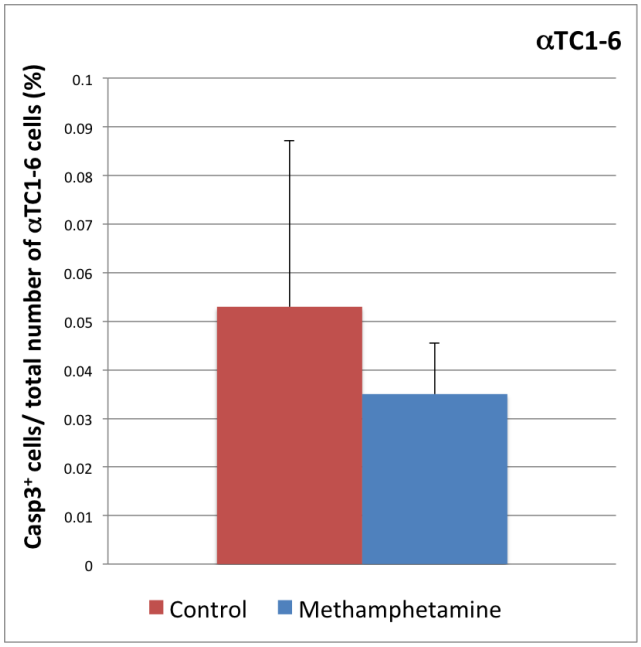

(c)

Figure 3.9: Representative confocal images of αTC1-6 cells in 20X magnification. The control group is shown in (a) and the methamphetamine treated cells are shown in (b). Immunosignal in green indicates Casp3-positive cells (a,b). Analysis of cell death (c) revealed no significant difference between methamphetamine-exposed cells and control group. Casp3-positive cells were normalized to total number of stained nuclei. Data are expressed as means ± S.D and statistical analysis was obtained by t-test. n = 3 coverslips per treatment. Scale bars 20μm.

3.4 Glucose level in the blood is elevated in offspring prenatally exposed to methamphetamine

To determine if mice prenatally exposed to methamphetamine show an alteration in glucose metabolism, GTT was performed in 6 week old offspring. Calculation of body weight revealed a significant increase in body weight of animals from methamphetamine treated mothers ($p < 0.01$). The quantification of body weight was conducted for both sexes and revealed a mean weight of 17 g in offspring prenatally exposed to saline and 19 g in offspring from methamphetamine treated mothers as shown in Fig.3.10. The area under curve (AUC), which shows changes in blood glucose level, showed significant increase of glucose level in the blood ($p < 0.05$) during GTT in 6 week old offspring prenatally exposed to methamphetamine with a mean value of $\approx$ 170mg/dl*min glucose in blood (Fig.3.12) compared to control with a mean value of $\approx$ 140mg/dl*min. GTT (Fig. 3.11) revealed that the baseline glucose level is higher in the methamphetamine compared to the saline group ($p < 0.001$). Analysis of blood glucose level after challenge showed that blood glucose levels are significant higher in mice from methamphetamine treated mothers compared to control (15 ($p < 0.01$), 30 ($p < 0.05$), 60 ($p < 0.01$), 90 ($p < 0.001$) and 120 ($p < 0.01$) minutes).

3.4 Glucose level in the blood is elevated in offspring prenatally exposed to methamphetamine

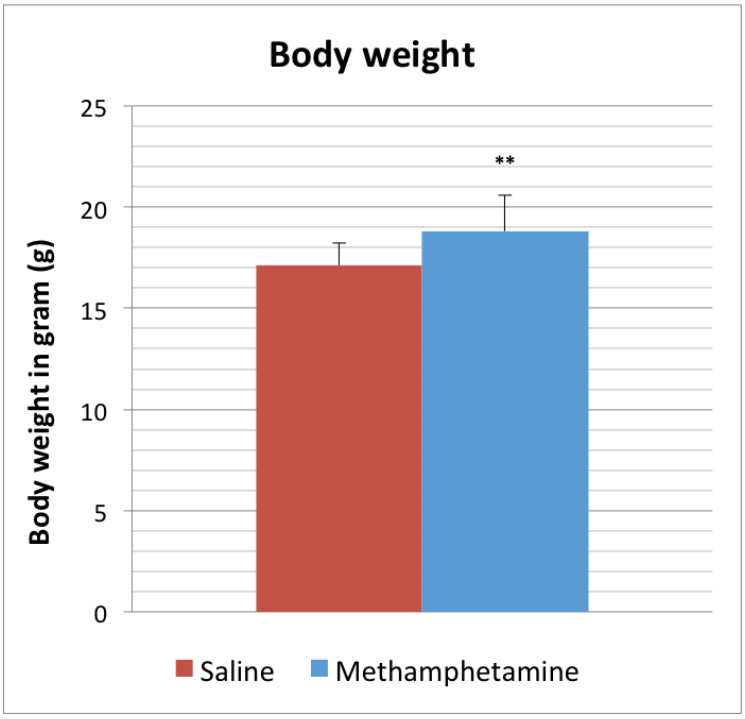

Figure 3.10: Quantification of body weight in gram from 6 week old mice prenatally exposed to methamphetamine and control mice. Data are expressed as means ± S.D and statistical analysis was obtained by t-test, **P <0.01. n = 16 animals per treatment were analyzed.

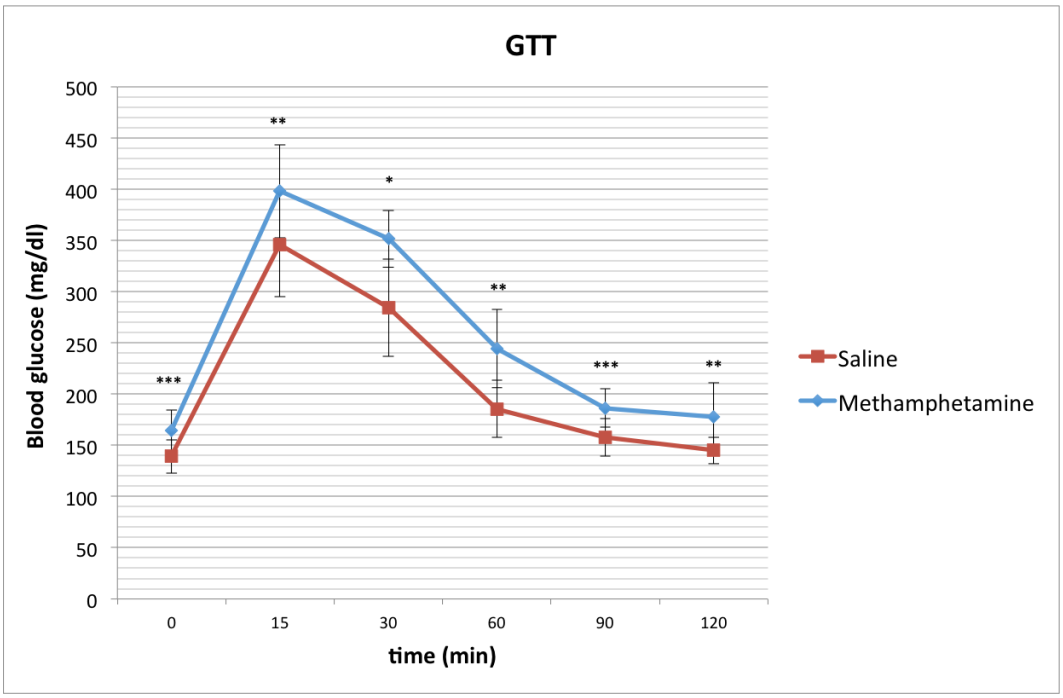

Figure 3.11: Analysis of blood glucose level before (0) and after glucose challenge (15, 30, 60, 90 and 120 minutes) from 6 week old offspring prenatally exposed to methamphetamine or saline. Data are expressed as means ± S.D and statistical analysis was obtained by t-test separately for each time point, ***P <0.001, **P <0.01, *P <0.05. n = 16 animals per treatment were analyzed.

3.4 Glucose level in the blood is elevated in offspring prenatally exposed to methamphetamine

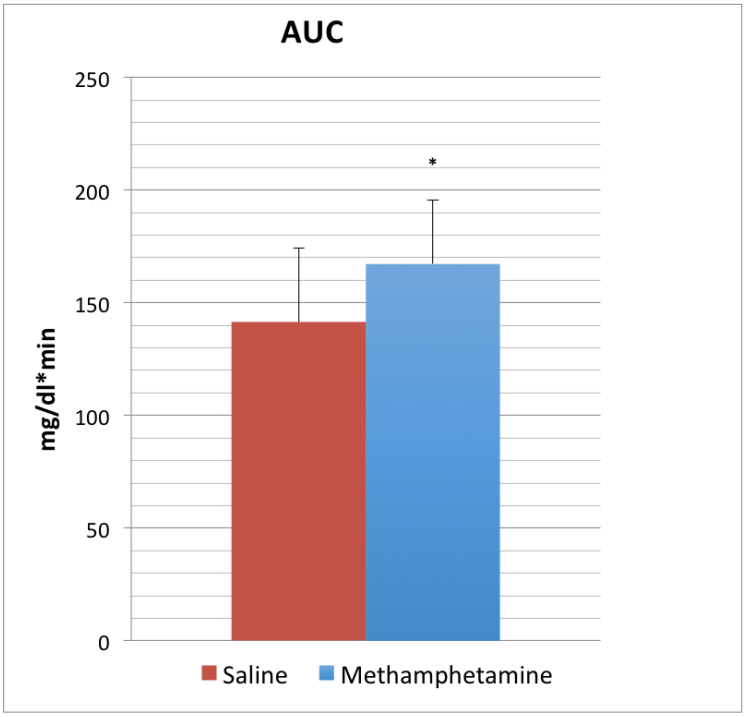

Figure 3.12: The area under the curve AUC revealed a significant increase in changes of blood glucose levels (mg/dl*min) during GTT in offspring from methamphetamine treated mice compared to control. Data are expressed as means ± S.D and statistical analysis was obtained by t-test, *P <0.05. n = 16 animals per treatment were analyzed.

3.5 Dopaminergic system is present in INS-1E and αTC1-6 cells

Glucose tolerance test showed that there is a significant change in blood glucose level in offspring from methamphetamine treated mothers. It is known that the effect of methamphetamine is influenced by the dopaminergic system in the brain. Because there is evidence of dopamine transporter, receptor and the vesicular monoamine transporter in the endocrine mouse pancreas we studied gene expression of *VMAT2*, *DAT*, *DRD2*, *DRD1* and *DRD3* in islets, INS-1E and αTC1-6 cell lines by PCR. Expression of *DRD2* was confirmed in αTC1-6 and INS-1E cell line (around 100 bp). *DRD1* gene expression was shown in αTC1-6 cells (Fig. 3.13). Neither, *VMAT2* nor *DRD3* showed PCR-products in INS-1E and αTC1-6 cells. Because a signal for DAT in αTC1-6 and *DRD1* in INS-1E cell line can not be excluded PCR was repeated for these genes and revealed in this second trial bands at around 50 bp in αTC1-6 cells for DAT and in INS-1E for *DRD1* (Fig.3.14).

3.6 Methamphetamine affects DRD1 gene expression in INS-1E cells

To examine if methamphetamine exposure affects *DRD1* and *DRD2* gene expression, PCR was conducted. *DRD1* gene expression in INS-1E cells

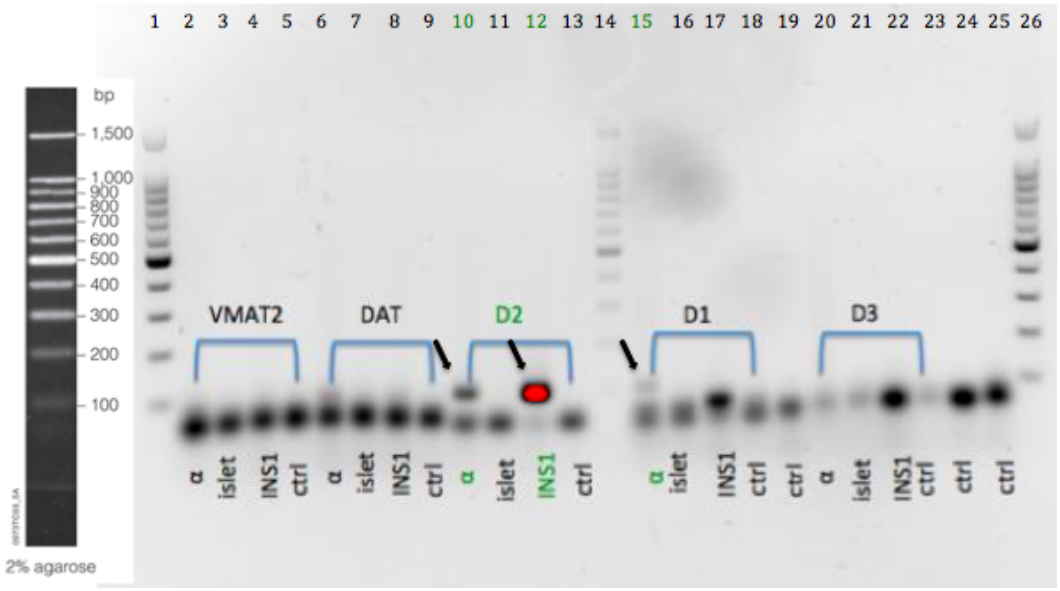

Figure 3.13: PCR analysis of *VAMT2*, *DAT*, *DRD2*, *DRD1* and *DRD3* gene expression in αTC1-6 cells (mouse), islets (mouse) and INS-1E cells (rat) revealed bands for *DRD2* gene expression in lane 10 and 12 and gene expression of *DRD1* in lane 15. For each primer pair a control without template was conducted. Lane 1, 14 and 26 indicate the DNA ladder with corresponding bp. Arrows show bands for *DRD2* in αTC1-6 and INS-1E and for *DRD1* in αTC1-6 cells.

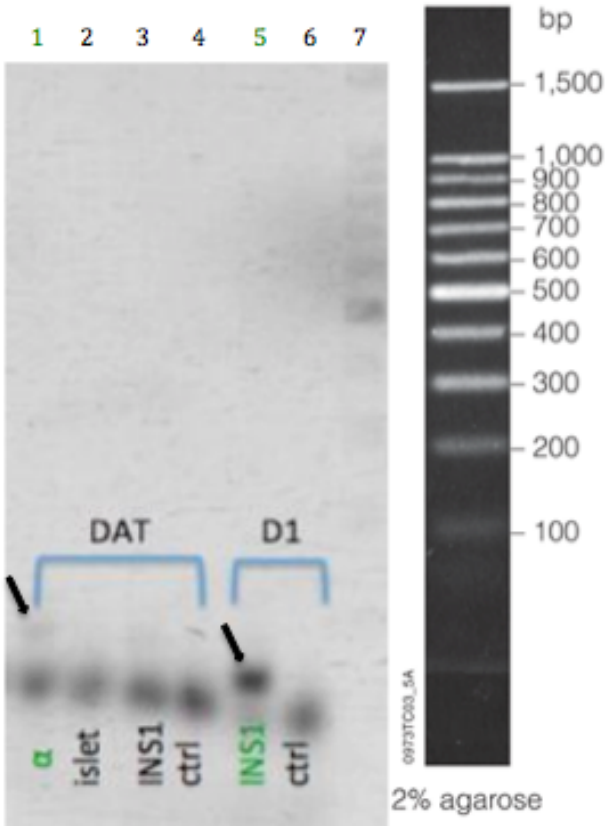

Figure 3.14: PCR analysis for *DAT* in αTC1-6 cells and *DRD1* in INS-1E cells show bands at around 50 bp.. For each pair of primers a control without genes was added. Lane 7 indicates the DNA ladder with corresponding bp. Arrows show bands of *DAT* and *DRD1* gene expression.

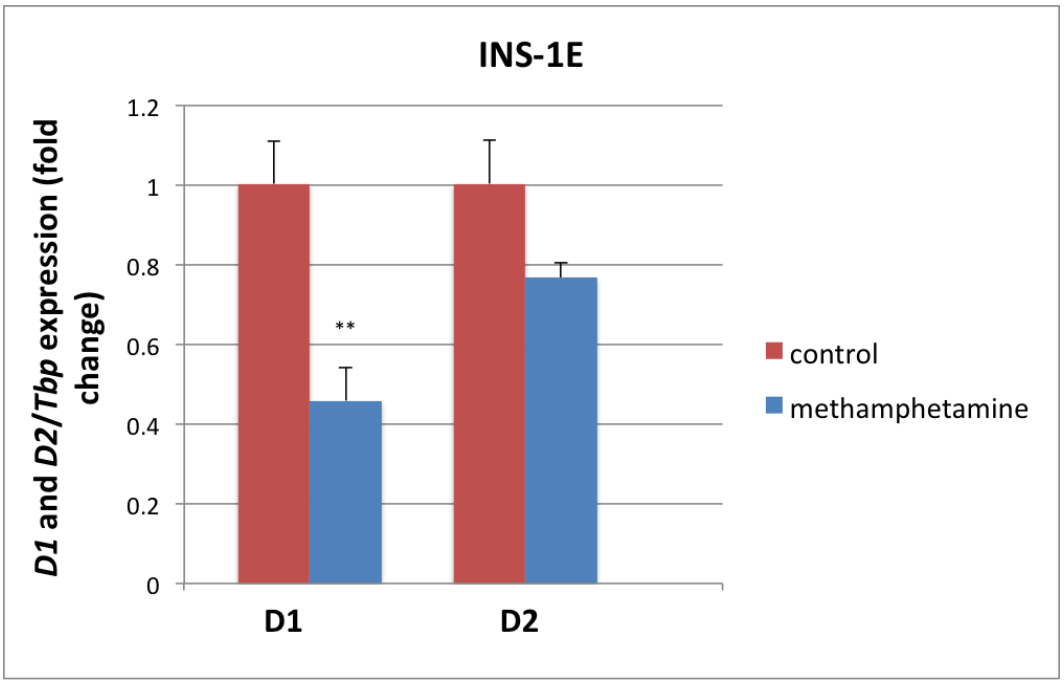

Figure 3.15: Quantification of *DRD1* and *DRD2* gene expression in either methamphetamine treated or control INS-1E cells. *DRD1* gene expression revealed a significant decrease in methamphetamine treated cells. Expression levels of *DRD1* and *DRD2* were normalized to *Tbp*. Data are expressed as means ± S.D, statistical analysis was obtained by t-test, **P <0.01.

revealed a significant decrease upon methamphetamine-exposure compared to the control group ($p < 0.01$). Expression of *DRD2* ($p \approx 0.0511$) in INS-1E (Fig. 3.15) as well as in αTC1-6 ($p \approx 0.2084$) (Fig.3.16) remained unaffected by methamphetamine treatment. Expression levels of *DRD1* and *DRD2* were normalized to *Tbp*.

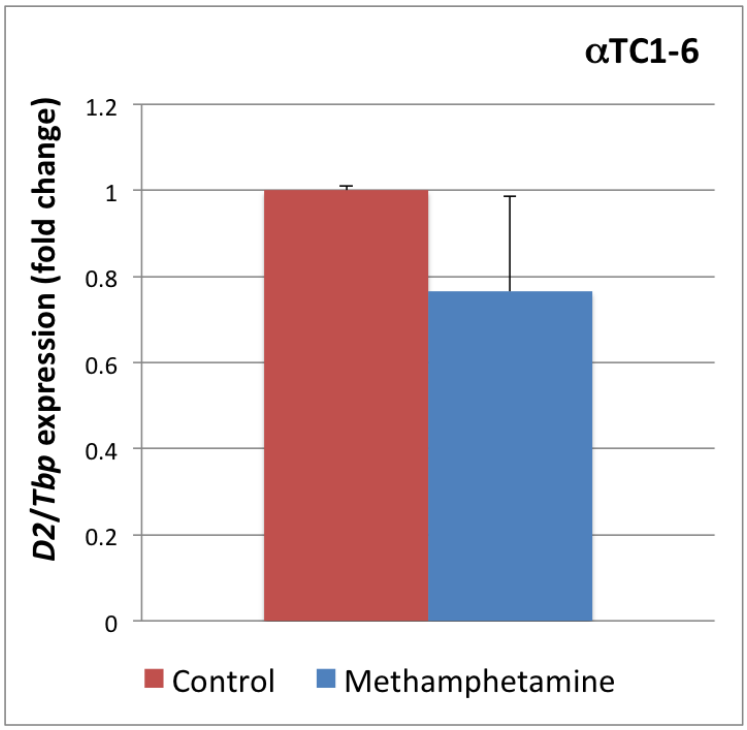

Figure 3.16: Analysis of *DRD2* gene expression in control and methamphetamine treated αTC1-6 cells. Expression levels of *DRD2* were normalized to *Tbp*. Data are expressed as means ± S.D, statistical analysis was obtained by t-test.

3.7 Dopamine transporter is present in α and β-cells in mouse pancreas

PCR analysis revealed *DAT* and *DRD2* expression in αTC1-6 cells as well *DRD2* expression in INS-1E cells. Therefore we performed immunohistochemistry to study if DAT and DRD2 are present in pancreatic α and β-cells of Po and 6 week old offspring prenatally exposed to saline. Although we did not detect *VMAT2* expression in INS-1E and αTC1-6 cell lines and pancreatic islets by PCR we wanted to examine if it is present in pancreata of Po. To distinguish between α and β-cells, co-immunostaining for insulin and glucagon was performed. Immunoreactivity of DAT in α and β-cells of 6 week old offspring from methamphetamine treated mothers can be confirmed (Fig.3.17b). Expression of *DRD2* in 6 week old offspring can not be confirmed. Further *VMAT2* was not detected neither on gene expression nor on protein level as demonstrated in Fig.3.17c & 3.17d.

3.8 Immunodetection of DAT in INS-1E cells

Due to the fact that DAT signal can be detected with immunostaining in β-cells of mouse pancreas we investigated if DAT protein can be detected in INS-1E cells. Western blot confirmed the presence of DAT as shown in Fig.3.18a. We measured protein level of DAT by Western blot in control and methamphetamine treated INS-1E cells, which revealed no significant

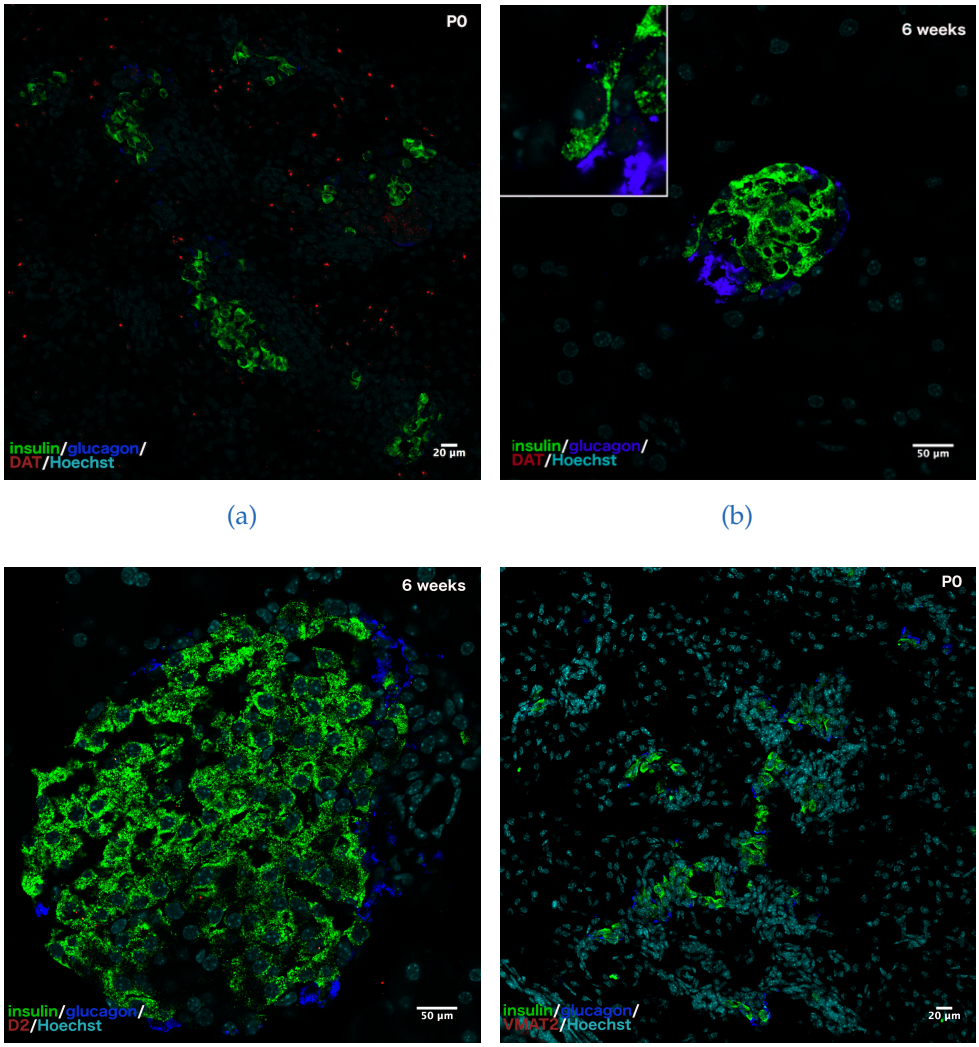

(a) (b)

(c) (d)

Figure 3.17: Representative confocal images of pancreatic tissue of P0 mice (20X magnification) and 6 week old offspring (40X magnification). Cells in green are positive for insulin, in blue positive for glucagon and in red positive for DAT. Nuclei were stained with Hoechst (pseudocolored in turquoise). Red signal is nonspecific in P0 exocrine pancreatic tissue (a). DAT reactivity is shown in α and β-cells of 6 week old offspring prenatally exposed to methamphetamine (b). There is no positive signal for DRD2 (c) in 6 week old offspring nor for VMAT2 (d) in P0. Scale bars 20μm for P0 and 50 μm for 6 weeks old.

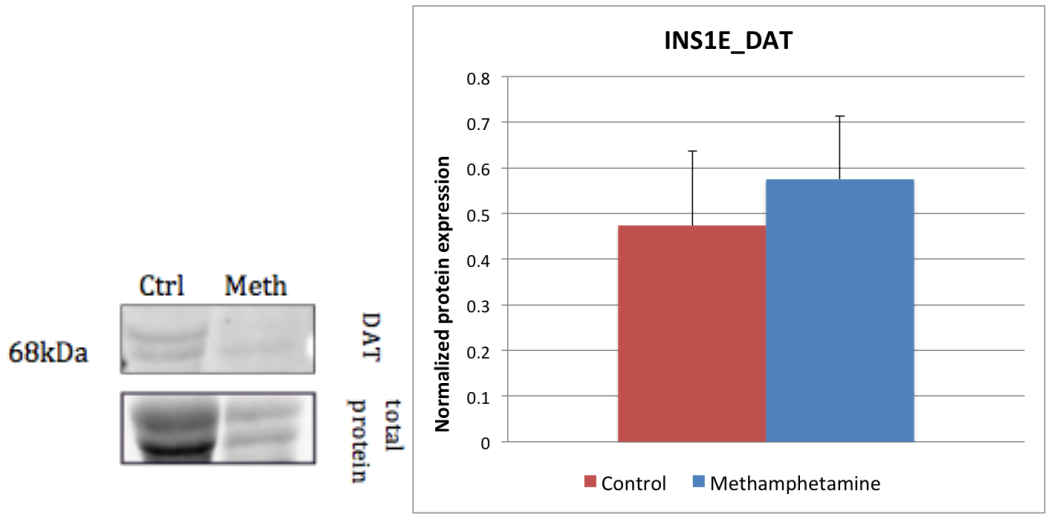

(a) (b)

Figure 3.18: Western blot analysis confirmed presence of DAT (68kDa) in INS-1E cells (a). DAT level is not significantly different between methamphetamine and control treated INS-1E cells (b). DAT protein level was normalized to total protein staining. Data are expressed as means ± S.D and statistical analysis was obtained by t-test. n = 3 values per treatment.

change (p = 0.5411) (Fig.3.18b). DAT protein staining was normalized to total protein staining.

4 Discussion

We wanted to examine if prenatal methamphetamine exposure affect insulin secretion hence glucose homeostasis. For this we focused on the dopaminergic signaling if this pathway is affected by methamphetamine. Our results revealed that methamphetamine influenced β-cell development in 6 week old offspring and showed an impaired glucose clearance in the blood. Additionally components of dopaminergic signaling in cell lines as well as in mouse islets were detected.

As quantitative analysis revealed that methamphetamine treatment does not influence the number of glucagon-positive α and insulin-positive β-cells in Po nor the number of glucagon-positive α cells in 6 week-old offspring. Instead only the number of insulin-positive β-cells is significantly decreased in 6 week old offspring prenatally exposed to methamphetamine compared to control. Indicating that an effect of methamphetamine on the number of β-cells is visible after some time. Yet, the number of islets in 6 week old offspring from methamphetamine treated mothers is significantly increased. The formation of islets is induced in the secondary transition at E13.5 [4]. In

the brain methamphetamine exposure triggers an increased Matrix metalloproteinases (MMP) activity. MMP's such as MMP2 and MMP9 that may be controlled by transforming growth factor (TGF)-β signaling are expressed during pancreas development [18]. *MMP2* expression in rats is highest at E17 and E19, during islet morphogenesis [23]. Methamphetamine application, at a time-point crucial for cell differentiation and islet formation, could affect TGF-β signaling activity hence alter cell islet formation. Investigations of methamphetamine treated mice on atherosclerosis showed that the cytokine TGF-β is significantly down regulated in these mice [42]. It is supposed that MMP and its inhibitors tissue inhibitors of metalloproteinases are involved in the degradation of extracellular matrix molecules like collagens, gelatins and laminins as well as in degradation of basal membrane hence regulating endocrine cell migration [18]. To maintain the glycemic level in both normal and pathophysiological states β-cell mass is dynamic, that encompass changes in rates of cell loss or death and changes in replication and neogenesis. [7] Within the first three weeks after birth the remodeling of islet architecture takes place that encompasses proliferation and apoptosis of cells to adjust to the metabolic needs [30]. Our results demonstrate that apoptosis of INS-1E cells is increased after exposure to methamphetamine. What remains unknown are the mechanisms that keep the cell number of α and β-cells in P0 from methamphetamine treated mothers unaffected. Bouwens et al.1994 [8] showed that in rat pancreas in the first 2 weeks after birth cytokeratin 20+ cells had higher bromodeoxyuridine incorporation than in regions composed of differentiated endocrine cells. Their findings indicate neogenesis, the process where new islets from progenitors or stem

cells are formed, in these duct epithelium cells [7].

It has been previously shown that in rats islet neogenesis can occur as late as at the age of 4 weeks [7]. Suggesting that the formation of endocrine cells and islets is still in process. Further investigations in mice at this stage could give information if there is a change in α and β-cell mass when prenatally exposed to methamphetamine.

Results from GTT showed that the glucose level in the blood is markedly higher and glucose clearance is decreased in offspring from methamphetamine treated mothers. These results could be explained by the decreased number of β-cells in 6 week old offspring. Additionally body weight of mice prenatally exposed to methamphetamine is significant higher compared to control. That could suggest that impaired glucose clearance could result from insulin insensitivity, which often accompanies increased body weight [24], [3]. An adequate β-cell mass should ensure a proper insulin secretion as a response to elevated glucose concentrations in the blood. The number of insulin-positive β-cells in Po is unaffected, what if these cells lost their ability to mature and still consist of immature properties. Immature cells have blunted GSIS as well as decreased low K_{ATP} resting conductance and high voltage-gated Ca^{2+} conductance and a monophasic insulin secretion [4].

The insulin response to an increased glucose level can be examined by the transcriptional and translational site of insulin synthesis. Insulin lost due to response to glucose must be replenished by resynthesis as an effect

of glucose-stimulated translation of pre-existing insulin mRNA molecules [19] or for the long term it depends on the stimulation of insulin gene transcription [16].

Immunohistochemistry of DAT and VMAT2 gave no ample evidence to be expressed in mouse P0 endocrine pancreas. As well there is no positive signal for DRD2 in pancreata of 6 week old mice in opposite to findings of Rubi et al. (2005). These differences could arise from experiments performed on mice with different weight. Additionally mice used for *DRD2* detection in experiments of Rubi et al. (2005) and our experiments came from different mouse strains. Only in 6 week old mouse DAT signal is detectable in α and β-cells. One can suppose that components necessary for dopamine synthesis and secretion are not needed at this early stage (P0) and that the neonatal β-cells of newborn still indicate immature properties. Given that one can hypothesize that dopaminergic components (i) are expressed in such a small amount not possible to detect with this technique or that these components (ii) are just activated and start being expressed with insulin synthesis and/or secretion [37].

It is known that islets express N-methyl-D-aspartate (NMDA) receptors and Marquard et al. [21] showed that inhibition of NMDA-R results in the increase of GSIS. NMDA-R support the influx of Ca^{2+} that triggers the opening of K^{+} channels which in turn leads to the repolarisation of the plasma membrane and decreases the influx of Ca^{2+} through VDCCs that results in a decreased exocytosis of insulin. Extracellular signal-regulated

kinase (ERK) plays a crucial role in cell proliferation, cell differentiation, cell death and survival [35]. ERK is also known to be a sensitive target for addictive drugs in the striatum and its psychostimulant-induced phosphorylation requires activation of DRD1 receptors [20]. PCR analysis of *DRD1* revealed its existence in INS-1E cells. Further qPCR shows that *DRD1* is under-expressed in INS1-E methamphetamine treated cells compared to control. Sun et al. [35] extended the influence of methamphetamine on ERK signaling via DRD1 and DRD2 receptors but also on NMDA receptors. Yeh et al. [41] revealed that high levels of dopamine block NMDA receptor channels in rat brains thus inhibit a NMDA receptor-mediated response. Via a ligand binding assay of (^{3}H)TCP the working group of Yeh found that the potential of this ligand to bind is decreased by methamphetamine exposure. Indeed this drug affects the NMDA signaling pathway but independently of dopamine. To test dopamine levels in glucose stimulated cells, dopamine as well as L-Dopa concentrations in the blood from methamphetamine treated mice could be measured before and after treatment with glucose. Taking together these findings of Marquad and Yeh who showed the connex between NMDA-Rs with insulin exocytosis and methamphetamine this could explain the results from the GTT that revealed impaired glucose homeostasis in animals prenatally exposed to methamphetamine.

The overall evidence for the dopaminergic network to exist in Po β-cells of mice can not be given in this study. On the one hand there is no signal of DAT, VMAT2 and DRD2 from immunohistochemistry and on the other hand the absence of *DRD1* and *DRD2* gene expression in mouse islets is

shown. Only immunohistochemistry could confirm DAT signal in 6 week old offspring in both α and β-cells. Results for DAT in cell lines from Western blot and qPCR gave no evidence to be significant different. If these results are gained due to low concentrations of these proteins one could use BCA-assay to detect small concentrations. Images from immunohistochemistry showed a bad image quality resulting in the disappearance of cells in the center of islets. This could be the result of bad freezing, sectioning, staining or mounting. For this immunohistochemistry should be repeated to gain a better quality of images useable for cell counting. Moreover one could use the adeno- associated virus vector to visualize DRD receptors like Ustione and Piston (2012) showed. [37] Further DRD2 should be immunolabeled also in P0 and VMAT2 in 6 weeks old to show if these proteins are present at different age.

Although Ustione and Piston (2012) [37] showed that dopamine act on insulin secretion and that methamphetamine can affect this pathway considering our results the drug itself can use other ways to negatively influence insulin secretion. As shown in prevoius papers ([35], [7] and [42]) methamphetamine has different ways to interact with transcription factors involved in development via its action on D2-like receptors, as well as factors involved in the transcription and translation of insulin synthesis. Also the secretion of insulin can be controlled by methamphetamine due its effect on NMDA receptors. Let's assume that another neurotransmitter is involved in glucose homeostasis. Bennet et al. (2016) [5] revealed that serotonin can regulate β-cell proliferation as well as insulin secretion. They observed the

expression and effect of serotonin receptor 5-HT_{2B} on insulin secretion in human and mouse β-cells.

Our studies demonstrate that methamphetamine affects glucose homeostasis in 6 week old offspring prenatally exposed to this drug. Still the way how the drug influence an adequate response to elevated glucose concentrations in the blood remains unclear and although DAT signal is present in 6 week old offspring other components of dopaminergic signaling seem to be absent in mouse β-cells.

Appendix

5 Abstrakt

Die korrekte Sekretion von Insulin als Reaktion auf eine erhöhte Glukose Konzentration im Blut ist wichtig um das Glukose Gleichgewicht aufrecht zu erhalten. Insulin wird in den β-Zellen der Langerhans'schen Inseln produziert und sezerniert. Die Dopamin Rezeptoren DRD1 und DRD2, der Dopamintransporter (DAT), der Vesikuläre Monoaminetransporter (VMAT2), L-3,4-dihydroxyphenylalanin (L-Dopa) und Dopamin wurden in den β-Zellen von Nagetieren nachgewiesen. Es wurde beobachtet, dass der Dopamin Signalweg durch Methamphetamin beeinflußt wird. Wir nehmen an, dass die Verabreichung von Methamphetamin zu einem bestimmten Zeitpunkt in der embryonalen Entwicklung Einfluß auf die Entwicklung des endokrinen Pankreas und der Langerhans'schen Insel hat und damit die adequate Insulinsekretion beeinflußt. Wir zeigen, dass die Anzahl der β-Zellen von Tieren welchen prenatal Methamphetamin verabreicht wurde, signifikant sinkt. Die Nachkommen der Methamphetamin behandelten Muttertiere zeigen ein erhöhtes Glukose Level im Blut zu Beginn und während des gesamten GTT. Weiters können wir zeigen, dass in der mit Methamphetamine behandelten INS-1E Zellen die Genexpression von *DRD1*

signifikant sinkt. In den 6 Wochen alten Nachkommen Methamphetamin behandelter Tiere nimmt die Anzahl der Insulin-positiven β-Zellen ab und wir untersuchten, ob dies durch Apoptosis hervorgerufen wird. Die Cleaved Caspase3 (Casp3) Immunofärbung zeigte, dass die Anzahl apoptotischer INS-1E Zellen durch eine Methamphetamin Exposition signifikant erhöht ist. Diese Resultate zeigen, dass Methamphetamin die Architektur der Langerhans'schen Inseln und die Genexpression von *DRD1* beeinflußt und eine nicht angemessene Reaktion auf eine erhöhte Glukosekonzentrationen im Blut zur Folge hat.

keywords: Glukose Gleichgewicht, Langerhans'sche Inseln, Insulin, β-Zellen, Dopamin Rezeptor 1, Dopamin Rezeptor 2, Dopamin Transporter, Vesikuläre Monoamine Transporter, Cleaved Caspase3, Methamphetamin

Bibliography

[1] J. Abel. Crystalline insulin. *PNAS; Proceedings of the National Academy of Sciences*, 12(2):132–136, 1926.

[2] A. M. Ahmed. History of diabetes mellitus. *Saudi medical journal*, 23(4):373–378, 2002.

[3] A. Assali, A. Ganor, Y. Beigel, Z. Shafer, T. Hershcovici, and M. Fainaru. Insulin resistance in obesity: body-weight or energy balance? *Journal of endocrinology*, 171(2):293–298, 2001.

[4] C. M. Benitez, W. R. Goodyer, and S. K. Kim. Deconstructing pancreas developmental biology. *Cold Spring Harbor perspectives in biology*, 4(6):a012401, 2012.

[5] H. Bennet, I. G. Mollet, A. Balhuizen, A. Medina, C. Nagorny, A. Bagge, J. Fadista, E. Ottosson-Laakso, P. Vikman, M. Dekker-Nitert, et al. Serotonin (5-ht) receptor 2b activation augments glucose-stimulated insulin secretion in human and mouse islets of langerhans. *Diabetologia*, 59(4):744–754, 2016.

[6] T. L. Blundell, J. Cutfield, E. Dodson, G. Dodson, D. Hodgkin, and D. Mercola. The crystal structure of rhombohedral 2 zinc insulin. In *Cold Spring Harbor symposia on quantitative biology*, volume 36, pages 233–241. Cold Spring Harbor Laboratory Press, 1972.

[7] S. Bonner-Weir, W.-C. Li, L. Ouziel-Yahalom, L. Guo, G. C. Weir, and A. Sharma. β-cell growth and regeneration: replication is only part of the story. *Diabetes*, 59(10):2340–2348, 2010.

[8] L. Bouwens, R.-N. Wang, E. De Blay, D. G. Pipeleers, and G. Klöppel. Cytokeratins as markers of ductal cell differentiation and islet neogenesis in the neonatal rat pancreas. *Diabetes*, 43(11):1279–1283, 1994.

[9] J. M. Brown, G. R. Hanson, and A. E. Fleckenstein. Methamphetamine rapidly decreases vesicular dopamine uptake. *Journal of neurochemistry*, 74(5):2221–2223, 2000.

[10] J. E. Bruin, L. D. Kellenberger, H. C. Gerstein, K. M. Morrison, and A. C. Holloway. Fetal and neonatal nicotine exposure and postnatal glucose homeostasis: identifying critical windows of exposure. *Journal of Endocrinology*, 194(1):171–178, 2007.

[11] J. D. Carter, S. B. Dula, K. L. Corbin, R. Wu, and C. S. Nunemaker. A practical guide to rodent islet isolation and assessment. *Biological procedures online*, 11(1):3, 2009.

[12] P. Collombat, A. Mansouri, J. Hecksher-Sørensen, P. Serup, J. Krull, G. Gradwohl, and P. Gruss. Opposing actions of arx and pax4 in

endocrine pancreas development. *Genes & development*, 17(20):2591–2603, 2003.

[13] L. Ericson, R. Håkanson, and I. Lundquist. Accumulation of dopamine in mouse pancreatic b-cells following injection of l-dopa. localization to secretory granules and inhibition of insulin secretion. *Diabetologia*, 13(2):117–124, 1977.

[14] S. J. Farnsworth, T. J. Volz, G. R. Hanson, and A. E. Fleckenstein. Cocaine alters vesicular dopamine sequestration and potassium-stimulated dopamine release: the role of d2 receptor activation. *Journal of Pharmacology and Experimental Therapeutics*, 328(3):807–812, 2009.

[15] A. E. Fleckenstein, R. R. Metzger, D. G. Wilkins, J. W. Gibb, and G. R. Hanson. Rapid and reversible effects of methamphetamine on dopamine transporters. *Journal of Pharmacology and Experimental Therapeutics*, 282(2):834–838, 1997.

[16] Z. Fu, E. R Gilbert, and D. Liu. Regulation of insulin synthesis and secretion and pancreatic beta-cell dysfunction in diabetes. *Current diabetes reviews*, 9(1):25–53, 2013.

[17] S. Hansen and C. Hedeskov. Simultaneous determination of the content of serotonin, dopamine, noradrenaline and adrenaline in pancreatic islets isolated from fed and starved mice. *Acta endocrinologica*, 86(4):820–832, 1977.

[18] S. K. Kim and M. Hebrok. Intercellular signals regulating pancreas development and function. *Genes & development*, 15(2):111–127, 2001.

[19] W. M. Macfarlane, S. B. Smith, R. F. James, A. D. Clifton, Y. N. Doza, P. Cohen, and K. Docherty. The p38/reactivating kinase mitogen-activated protein kinase cascade mediates the activation of the transcription factor insulin upstream factor 1 and insulin gene transcription by high glucose in pancreatic β-cells. *Journal of Biological Chemistry*, 272(33):20936–20944, 1997.

[20] L.-M. Mao, J. M. Reusch, E. E. Fibuch, Z. Liu, and J. Q. Wang. Amphetamine increases phosphorylation of mapk/erk at synaptic sites in the rat striatum and medial prefrontal cortex. *Brain research*, 1494:101–108, 2013.

[21] J. Marquard, S. Otter, A. Welters, A. Stirban, A. Fischer, J. Eglinger, D. Herebian, O. Kletke, M. S. Klemen, A. Stožer, et al. Characterization of pancreatic nmda receptors as possible drug targets for diabetes treatment. *Nature medicine*, 21(4):363–372, 2015.

[22] G. Mellitzer, S. Bonné, R. F. Luco, M. Van De Casteele, N. Lenne-Samuel, P. Collombat, A. Mansouri, J. Lee, M. Lan, D. Pipeleers, et al. Ia1 is ngn3-dependent and essential for differentiation of the endocrine pancreas. *The EMBO journal*, 25(6):1344–1352, 2006.

[23] F. Miralles, T. Battelino, P. Czernichow, and R. Scharfmann. Tgf-β plays a key role in morphogenesis of the pancreatic islets of langerhans by controlling the activity of the matrix metalloproteinase mmp-2. *The Journal of cell biology*, 143(3):827–836, 1998.

[24] P. Muzzin, R. C. Eisensmith, K. C. Copeland, and S. L. Woo. Correction of obesity and diabetes in genetically obese mice by leptin gene therapy. *Proceedings of the National Academy of Sciences*, 93(25):14804–14808, 1996.

[25] E. J. Nestler. The neurobiology of cocaine addiction. *Science & practice perspectives*, 3(1):4, 2005.

[26] J. R. Nickell, K. B. Siripurapu, A. Vartak, P. A. Crooks, and L. P. Dwoskin. The vesicular monoamine transporter-2: an important pharmacological target for the discovery of novel therapeutics to treat methamphetamine abuse. *Advances in pharmacology (San Diego, Calif.)*, 69:71, 2014.

[27] A. C. Powers, S. Efrat, S. Mojsov, D. Spector, J. F. Habener, and D. Hanahan. Proglucagon processing similar to normal islets in pancreatic α-like cell line derived from transgenic mouse tumor. *Diabetes*, 39(4):406–414, 1990.

[28] J. H. Pratt. A reappraisal of researches leading to the discovery of insulin. *Journal of the History of Medicine and Allied Sciences*, pages 281–289, 1954.

[29] B. Rubí, S. Ljubicic, S. Pournourmohammadi, S. Carobbio, M. Armanet, C. Bartley, and P. Maechler. Dopamine d2-like receptors are expressed in pancreatic beta cells and mediate inhibition of insulin secretion. *Journal of Biological Chemistry*, 280(44):36824–36832, 2005.

[30] J. M. Rukstalis and J. F. Habener. Neurogenin3: a master regulator of pancreatic islet differentiation and regeneration. *Islets*, 1(3):177–184, 2009.

[31] Y. Seino, K. Nanjo, N. Tajima, T. Kadowaki, A. Kashiwagi, E. Araki, C. Ito, N. Inagaki, Y. Iwamoto, M. Kasuga, et al. Report of the committee on the classification and diagnostic criteria of diabetes mellitus. *Journal of diabetes investigation*, 1(5):212–228, 2010.

[32] P. A. Seymour and M. Sander. Historical perspective: Beginnings of the β-cell. *Diabetes*, 60(2):364–376, 2011.

[33] M. Skelin, M. Rupnik, and A. Cencic. Pancreatic beta cell lines and their applications in diabetes mellitus research. *Altex*, 27(2):105–113, 2010.

[34] T. Sun, J. Guo, H. Chen, J. Zhang, X. Zhang, X. Jiang, F. Wang, Z. Xu, X. Huang, J. Sha, et al. Maternal caffeine exposure impairs insulin secretion by pancreatic β-cells and increases the risk of type ii diabetes mellitus in offspring. *Cell biology international*, 38(10):1183–1193, 2014.

[35] W.-L. Sun, P. M. Quizon, and J. Zhu. Chapter one-molecular mechanism: Erk signaling, drug addiction, and behavioral effects. *Progress in molecular biology and translational science*, 137:1–40, 2016.

[36] G. Szot. Murine pancreatic islet isolation, October 2017.

[37] A. Ustione and D. W. Piston. Dopamine synthesis and d3 receptor activation in pancreatic β-cells regulates insulin secretion and intracellular [ca2+] oscillations. *Molecular endocrinology*, 26(11):1928–1940, 2012.

[38] A. Ustione, D. W. Piston, and P. E. Harris. Minireview: dopaminergic regulation of insulin secretion from the pancreatic islet. *Molecular endocrinology*, 27(8):1198–1207, 2013.

[39] I. Von Mering. Diabetes mellitus nach pancreas extirpation. *Zentral Klin. Medzin*, 10:394, 1889.

[40] W. W. Web. Western blot system, 2018.

[41] G.-C. Yeh, J.-C. Chen, H.-C. Tsai, H.-H. Wu, C.-Y. Lin, P.-C. Hsu, and Y.-C. Peng. Amphetamine inhibits then-methyl-d-aspartate receptor-mediated responses by directly interacting with the receptor/channel complex. *Journal of Pharmacology and Experimental Therapeutics*, 300(3):1008–1016, 2002.

[42] P. Zhu, L. Li, B. Gao, M. Zhang, Y. Wang, Y. Gu, and L. Hu. Impact of chronic methamphetamine treatment on the atherosclerosis formation

in apoe-/- mice fed a high cholesterol diet. *Oncotarget*, 8(33):55064, 2017.